

**CRYOGENIC SEPARATION OF CO<sub>2</sub> FROM METHANE  
USING DYNAMIC PACKED BED**

By

Nor Syahera Binti Mohamad

Dissertation submitted in partial fulfillment of the requirements for the

Bachelor of Engineering (Hons)

(Chemical Engineering)

MAY 2012

Universiti Teknologi PETRONAS

Bandar Seri Iskandar

31750 Tronoh

Perak Darul Ridzuan

**CERTIFICATION OF APPROVAL**

**CRYOGENIC SEPARATION OF CO<sub>2</sub> FROM METHANE  
USING DYNAMIC PACKED BED**

By

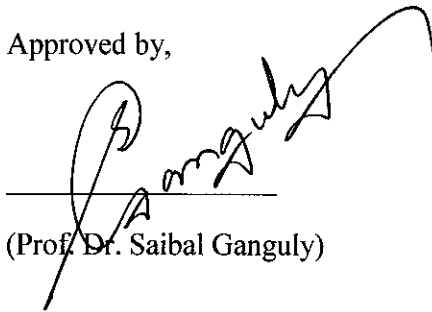
Nor Syahera Binti Mohamad

Dissertation submitted in partial fulfillment of the requirements for the

**BACHELOR OF ENGINEERING (Hons)**

**(CHEMICAL ENGINEERING)**

Approved by,

A handwritten signature in black ink, appearing to read 'Saibal Ganguly', is written over a horizontal line. The signature is cursive and extends upwards and to the right.

(Prof. Dr. Saibal Ganguly)


UNIVERSITI TEKNOLOGI PETRONAS

TRONOH, PERAK

May 2012

## CERTIFICATION OF ORIGINALITY

This is to certify that I am responsible for the work submitted in this project, that the original work is my own except as specified in the references and acknowledgements, and that the original work contained herein have not been undertaken or done by unspecified sources or persons.

 5/9/2012

---

NOR SYAHERA BINTI MOHAMAD

## ABSTRACT

The high content of carbon dioxide in the natural gas is a major concern in harnessing the natural gas. This is due to the acidity of the carbon dioxide which will impose problem to the extraction, production and transportation of the natural gas. Cryogenic separation of carbon dioxide from natural gas is proposed to separate carbon dioxide from the high carbon dioxide content natural gas using the dynamic packed bed. An effective separation between the carbon dioxide and methane can be obtained using the cryogenic packed bed. This separation is possible due to the difference in dew and sublimation points of carbon dioxide and methane. This is because, due to the sublimation point of carbon dioxide which is  $-78.5^{\circ}\text{C}$  which is at higher temperature than methane, which is  $-182^{\circ}\text{C}$ , the carbon dioxide will deposit on the packing material at temperature below its sublimation point. Carbon dioxide is depositing on the packing material by the transfer of the cold energy which is stored in the packing material. The carbon dioxide molecule is cooled from the transfer of energy from the cold material (packing material) to the hot material (carbon dioxide) and deposited onto the packing material. Methane will not be deposited and will flow freely out of the bed as there are empty spaces inside the packed bed. Mathematical analysis was performed to better understand the separation characteristic of carbon dioxide from methane and experiments are to be carried out for cryogenic  $\text{CO}_2$  capture. From the mathematical analysis, the mass deposition rate of the carbon dioxide is found out to be increasing sharply as the concentration of carbon dioxide increases. The dynamic behavior of the packed bed is described using the one dimensional plug flow model.

## ACKNOWLEDGEMENTS

First and foremost, the author desires to express his warmest gratitude to his Final Year Project supervisor, Prof Dr. Saibal Ganguly, for having been very helpful and encouraging. From the start of the project, he has been giving guidance from the smallest detail. He has taught how to conduct proper research, starting from the inception through practical hands-on, on to the presentation of findings. He has instilled in the author the sense of team work, good communication skills and project management.

Secondly, the author would like to express his appreciation to the laboratory technicians in the Chemical Engineering Department, from Block 3, Block 4, and Block 5. To name a few are Mr. Shahanizam, Mr. Firdaus, Mr. Jailani Mr. Fauzi and Mr. Saharudin and the rest. They have been providing the author with assistance, technical knowledge and resources which are much needed to complete the project. Their aids have been a good push to the project.

Not to forget the author's team mates: Mr. Dhanaraj, Mr. Abu Ghaly, Mr. Abul Hasan and Dr. Jayita Pal. They have assisted physically as well as in providing the means to achieve the goal. They have also provided consultations and ideas to further the cause.

## TABLE OF CONTENTS

|  |            |
|--|------------|
| <b>CERTIFICATION</b> .....   | <b>i</b>   |
| <b>ABSTRACT</b> .....  | <b>iii</b> |
| <b>ACKNOWLEDGEMENT</b> .....   | <b>iv</b>  |
| <b>CHAPTER 1: INTRODUCTION</b> .....   | <b>1</b>   |
| 1.1 Background Study.....  | 1          |
| 1.2 Problem Statement.....   | 2          |
| 1.3 Objectives.....  | 3          |
| 1.4 Scope of Study.....  | 3          |
| <b>CHAPTER 2: LITERATURE REVIEW</b> .....  | <b>4</b>   |
| 2.1 Process Principle.....   | 10         |
| 2.2 Characterization of feed and product.....  | 14         |
| <b>CHAPTER 3: RESEARCH METHODOLOGY</b> .....   | <b>17</b>  |
| 3.1 Mathematical Analysis.....   | 18         |
| 3.2 Experimental Study on the Cryogenic CO <sub>2</sub> Capture Using<br>Dynamic Packed Bed..... | 19         |
| 3.3 Gantt Chart.....   | 25         |
| <b>CHAPTER 4: RESULT AND DISCUSSION</b> .....  | <b>27</b>  |
| 4.1 Methodology of the Simulation.....   | 27         |
| 4.2 Experimental Study On The Cryogenic CO <sub>2</sub> Capture Using<br>Dynamic Packed Bed..... | 28         |
| <b>CHAPTER 5: CONCLUSION AND RECOMENDATION</b> .....   | <b>46</b>  |
| 5.1 Recommendation.....  | 46         |
| 5.2 Conclusion.....  | 47         |
| <b>REFERENCES</b> .....  | <b>48</b>  |
| <b>APPENDIX</b> .....  | <b>49</b>  |

## LIST OF FIGURE

|   |    |
|---|----|
| Figure 1: Solid CO <sub>2</sub> formed on the packing material (M. J. Tuinier, et al., 2010) .....  | 6  |
| Figure 2: Schematic axial temperature and corresponding mass deposition<br>profiles for the capture (a), recovery (b), and cooling (c) cycle respectively ..... | 7  |
| Figure 3: Schematic diagram for cryogenic CO <sub>2</sub> capture system based on<br>stirling coolers.....  | 8  |
| Figure 4: Operational zones of the CFZ technology .....   | 9  |
| Figure 5: Pressure–temperature relations for carbon dioxide-methane System.....   | 10 |
| Figure 6: Temperature-composition section system at 673 psia .....  | 11 |
| Figure 7: Carbon dioxide – methane system phase diagram for pressure of 673 psia ....   | 12 |
| Figure 8: Schematic illustration of the process concept: (a) and (b) during the capture<br>Step, (c) and (d) during the recovery step .....                     | 13 |
| Figure 9: Example of peaks from gas chromatograph .....   | 14 |
| Figure 10: Calibration curve for methane .....  | 14 |
| Figure 11: Calibration curve for carbon dioxide.....  | 15 |
| Figure 12: Schematic diagram of packed bed with axial flow .....  | 15 |
| Figure 13: Packed bed properties .....  | 28 |
| Figure 14: The experimental set up for the cryogenic separation of<br>CO <sub>2</sub> and CH <sub>4</sub> from natural gas with the gas cylinders.....          | 19 |
| Figure 15: Complete setup of the cryogenic capture of CO <sub>2</sub> .....   | 19 |
| Figure 16: Gas Chromatography Flame Ionization Detector: SHIMADZU GC-20101<br>with the item code: GC-CE-04.....   | 20 |
| Figure 17: Gas sampling bag containing pure CO <sub>2</sub> , pure CH <sub>4</sub> and a mixture<br>of 60% CO <sub>2</sub> and 40% CH <sub>4</sub> . .....      | 21 |
| Figure 18: Micro syringe for sample extraction .....  | 21 |
| Figure 19: Experimental set up of cryogenic CO <sub>2</sub> separation .....  | 24 |
| Figure 20: The curve generated for the change in percentage of CO <sub>2</sub><br>in the z direction for the different time. ....                               | 33 |
| Figure 21: The curve generated from energy balance for change in<br>temperature of packed bed in the z direction for different time t.....                      | 34 |

|   |    |
|---|----|
| Figure 22: Mass deposition rate versus temperature.....   | 35 |
| Figure 23: Result from a known sample analysis using gas chromatograph .....  | 36 |
| Figure 24: Calibration Curve for Carbon Dioxide .....   | 37 |
| Figure 25: Calibration Curve for Methane.....   | 37 |
| Figure 26: The condition set for the gas chromatography .....   | 38 |
| Figure 27: The condition set for the gas chromatography (oven) .....  | 39 |
| Figure 28: Study of the heat loss to the surrounding of the system .....  | 41 |
| Figure 29: Temperature profile for the CO <sub>2</sub> capture using packed bed .....   | 42 |
| Figure 30: The location of the thermometer probes.....  | 43 |
| Figure 31: Gas Chromatography result for case 1 .....   | 44 |
| Figure 32: Gas Chromatograph result for case 2 .....  | 45 |
| Figure 33: Temperature profile for the CO <sub>2</sub> capture using packed bed with bed<br>composite cooling & capture data..... | 45 |



## LIST OF TABLE

|  |    |
|--|----|
| Table 1: Conditions and coefficients values used in the numerical studies .....                    | 28 |
| Table 2: Mass deposition rate at different temperature for different CO <sub>2</sub> concentration | 31 |
| Table 3: Bed Void Fraction.....  | 39 |
| Table 4: Cryogenic Packed Bed Properties.....  | 40 |
| Table 5: Result from experiment cryogenic CO <sub>2</sub> capture using packed bed .....           | 44 |

## NOMENCLATURE

|               |  |
|---------------|--|
| $A$           | Heat transfer area of the surface, $m^2$                               |
| $a_s$         | Specific solid surface area per unit bed volume, $m^2/m^3$             |
| $C_{p_g}$     | Heat capacity, J/kg.K  |
| $CO_2$        | Carbon dioxide   |
| $CH_4$        | Methane  |
| $D_{eff}$     | Effective diffusion coefficient, $m^2/s$                               |
| $d_p$         | Particle diameter, m   |
| $g$           | Mass deposition rate constant, s/m                                     |
| $h$           | Convective heat transfer coefficient, $W/m^2K$                         |
| $L$           | Bed length, m  |
| $\dot{m}_i^n$ | Mass deposition rate per unit surface area for component i, $kg/m^2/s$ |
| $n_c$         | Number of components   |
| $Nu$          | Nusselt number   |
| $P_a$         | Parameter in axial heat dispersion coefficient                         |
| $P$           | Pressure, Pa   |
| $Pe_{ax}$     | Peclet number for axial heat dispersion                                |
| $Pr$          | Prandtl number   |
| $q$           | Heat transferred per unit time, W                                      |
| $Re$          | Reynolds number  |
| $Sc$          | Schmidt number   |
| $t$           | Time, s  |
| $T$           | Temperature of gas mixture, K  |
| $V_{bed}$     | Volume of bed, $m^3$   |
| $v_g$         | Superficial velocity, m/s  |

|     |                        |
|-----|------------------------|
| $y$ | Mole fraction, mol/mol |
| $z$ | Axial coordinate, m    |
| GC  | Gas chromatograph      |

### **Greek Letters**

|                   |  |
|-------------------|--|
| $\Delta h_i$      | Enthalpy change related to the phase change of component i, j/kg |
| $\varepsilon_g$   | Bed void fraction  |
| $\mu$             | Viscosity, kg/m/s  |
| $\lambda_g$       | Mixture thermal conductivity, W/mK                               |
| $\lambda_{bed,0}$ | Effective bed conductivity at no flow conditions, W/mK           |
| $\lambda_{eff}$   | Effective conductivity, W/mK                                     |
| $\rho$            | Density, kg/m <sup>3</sup>                                       |

### **Subscripts**

|     |             |
|-----|-------------|
| $g$ | Gas phase   |
| $s$ | Solid phase |
| $i$ | component   |

## CHAPTER 1

### INTRODUCTION

#### 1.1. Background Study

It is important to know that the consumption of natural gas worldwide is forecasted to increase by more than 90 per cent by year 2030 (Malaysia, 2011). As of currently, there are 25 power plants in Malaysia that is operated using the natural gas compared with only 1 power plant in 1984. This shows the increasing demand of natural gas. However, the depleting natural gas reserve is of worldwide concern. Moreover, the new uneconomic field has high CO<sub>2</sub> content ranging from 12% to 40% (Malaysia, 2011), and the CO<sub>2</sub> content in the Malaysian natural gas which can reach up to 80%. Besides that according to (Hart & Gnanendran, 2009) the LaBarge gas field in SW Wyoming (USA) which has 65% of CO<sub>2</sub> was discovered in 1963, but the production of the field is delayed until 1986 due to high CO<sub>2</sub> concentration. The high content of CO<sub>2</sub> may cause corrosion problem in extraction, transportation, production of the natural gas (S.A. Enbenzer, 2005). Besides that, CO<sub>2</sub> also poses a threat to the environment as it is one of the major greenhouse gases (Fleay, 2002). Therefore, efficient separation of CO<sub>2</sub> is a must. It is important to research for technologies that can be easily applied in the offshore platform due to the limitations that must be complied with the offshore platform such as lack of space and materials.

Therefore, it is suggested to perform the cryogenic separation of CO<sub>2</sub> from natural gas. This is because; this method is suitable for the separation of high content of CO<sub>2</sub> (Hart & Gnanendran, 2009). Other method such as the amine scrubbing is only suitable for CO<sub>2</sub> content from 3% to 25% (Keskes, Adjiman, Galindo, & Jackson, 2006) because the degree of absorption is restricted to the fixed stoichiometry of the chemical reaction. While membrane process possesses high potential for a wide range of CO<sub>2</sub> content, it is

prone to rupture at high pressure and may cause other operational problem. This is not tolerable in the offshore platform due to location and cost of operation. Slight problem that can delay the production may cause billions to be lost. Besides that the application of the cryogenic separation process is simple and can eliminate the need for solvent regeneration. The separation method using the dynamic packed bed for simultaneous separation of CO<sub>2</sub> and H<sub>2</sub>O from natural gas is proposed to separate the high CO<sub>2</sub> content in the natural gas.

### **1.2.Problem Statement**

The project is carried out to study the characteristic of separation of CO<sub>2</sub> from natural gas using the recently developed technology for the separation of CO<sub>2</sub> from flue gas. The cryogenic dynamic packed bed is an interesting model that can be studied to be used for the separation of CO<sub>2</sub> from natural gas. This is because; the technology is employing the cryogenic condition to separate the CO<sub>2</sub> without applying any absorbent. This is a good point to be noted as the regeneration of the absorbent will consume a lot of energy thus require higher cost (Davidson & Kelly, 2004). As it is just recently developed, the technology is not tested using the natural gas as feed. Therefore, it will be beneficial if the technology is tested to be suitable to be used for the separation of CO<sub>2</sub> from natural gas.

However, the problem statement for this project is closely related to the problems of using the cryogenic separation process. According to (Song, Kitamura, Li, & Ogasawara, 2012a), the drawback of the cryogenic separation process include the plugging of the system by ice which will then require more cost for dehydration of the feed stream before entering the cryogenic separation system. Thus extra cost needs to be invested for separate removal of water.

### **1.3.Objectives**

The objective of this project is listed as follows:

- Preliminary research for cryogenic separation using dynamic packed bed for separation of CO<sub>2</sub> and CH<sub>4</sub> in natural gas.
- To investigate the space and time variation of weight fraction and mass deposition of CO<sub>2</sub> in the packed bed using mathematical analysis.

### **1.4.Scope of study**

The scope of this project is as a preliminary research on the cryogenic CO<sub>2</sub> capture using dynamically operated packed beds technology by (M. J. Tuinier, et al., 2010) in simultaneous separation of CO<sub>2</sub> and H<sub>2</sub>O from natural gas. The project is focusing on the capture cycle where the cryogenic separation using dynamic packed bed for separation of CO<sub>2</sub> and H<sub>2</sub>O from natural gas is investigated. Besides that, it is also important to investigate the separation characteristic of CO<sub>2</sub> and H<sub>2</sub>O from natural gas in the capture cycle. During the study, mathematical analysis on the mass deposition of CO<sub>2</sub> during the separation is performed. Besides that, experimental study will also be carried out to obtain the match and verification of simulation results. The designing and procuring for the experiment is also carried out to obtain all the needed equipment as this project is still in the early stages and not much equipment is available for cryogenic experiment.

## **CHAPTER 2**

### **LITERATURE REVIEW**

#### **2. LITERATURE REVIEW**

There are plenty of process and method currently used, developed or under development around the world to solve the problem of separating the CO<sub>2</sub> from the desired end product. The technologies involved in the CO<sub>2</sub> separation is adsorption, absorption, cryogenic and membrane (Song, Kitamura, Li, & Ogasawara, 2012b). Some of these method or processes can be applied to the separation of CO<sub>2</sub> from natural gas with further modifications. There are plenty of problems related to CO<sub>2</sub> separation or capture. This includes high energy consumptions due to the need to regenerate the absorbents used or due to the need to recompressed the flue gas streams for operations at elevated pressure (M.J. Tuinier, M. van Sint Annaland, G.J. Kramer, & J.A.M. Kuipers, 2010). The separation process must be able to reduce the amount of CO<sub>2</sub> to a desirable level which is different for each country. However, the level of CO<sub>2</sub> and other contaminant or more commonly known as the specs for the natural gas pipeline is less than or equal to 2% to 4 % of CO<sub>2</sub> and less than 4ppm of H<sub>2</sub>S (Hart & Gnanendran, 2009). This specification must be complied to ensure smooth transportation of natural gas as high content of the acid gases such as CO<sub>2</sub> and H<sub>2</sub>S will corrode the pipeline. Besides that, high concentration of acid gases will also hinder the production and extraction of the natural gas. Therefore efforts are taken to research for technology that are suitable to be used to separate the acid gases from the natural gas. For example, several methods involving cryogenic separation of CO<sub>2</sub> is developed and published. However, the process is not extensively studied to the high cost of refrigeration (Davidson & Kelly,

2004). Even more so, researchers are not giving up on the idea of cryogenic separation of CO<sub>2</sub> from natural gas. This is prominent in the previous and recent work published which is focusing on solving the problem related to the cryogenic separation technology using different method. Such work done by Tuinier M.J., and et al., suggest exploiting the cold duty at the site to counter the expensive refrigeration which is used in the cryogenic process. This will significantly reduce the high energy consumption needed in the process. Moreover, the cryogenic process can dismiss the use of absorbents thus eliminating the need to regenerate the absorbents. Regenerating the absorbents is a costly process due to the high energy required.

Currently there are a few novel processes implementing the use of cryogenic condition in separating the CO<sub>2</sub> from the flue gas or natural gas. The first technology that is to be reviewed here is a cryogenic separation technology recently published which is the work done by (M. J. Tuinier, et al., 2010) titled: Cryogenic CO<sub>2</sub> Capture Using Dynamically Operated Packed Beds. This technology makes use of the difference in the dew point and sublimation point which will enable the separation of CO<sub>2</sub> from flue gas. It is important to note that, desublimation or deposition is the phase change from gaseous form to the solid phase which is in contra with the term sublimation which means phase change from solid phase to gaseous phase. The plugging problem often occur in the cryogenic separation technology is minimized as the CO<sub>2</sub> is desublimated or deposited onto the packing material, thus the gas can flow freely without obstruction using the technology. M. J. Tuinier, et al., 2010 had used packed bed column filled with spherical glass particles which acts as the deposition particle for the CO<sub>2</sub> to avoid the plugging of the column. As the solid CO<sub>2</sub> is deposited onto the packing material, there will be empty spaces or void spaces for the gases to flow to the end of the bed. This is shown in the figure 1. Finally the solid CO<sub>2</sub> that are captured inside the bed must be recovered outside of the bed; therefore, a pure gaseous CO<sub>2</sub> stream is then fed into the column. The pure gaseous CO<sub>2</sub> will increase the partial pressure of CO<sub>2</sub> and this will allow the solid CO<sub>2</sub> to melt into liquid form and to be collected in a liquid form.



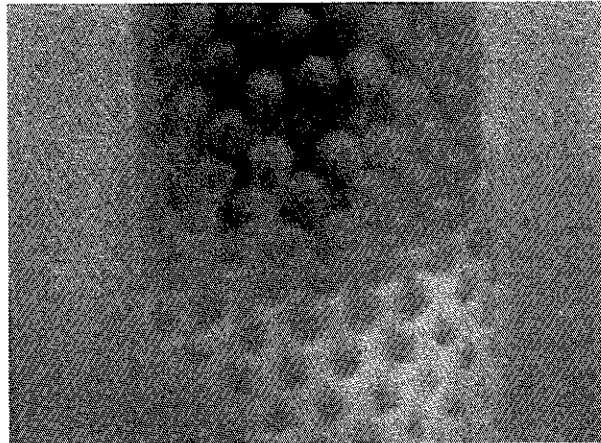


Figure 1: Solid CO<sub>2</sub> formed on the packing material (M. J. Tuinier, et al., 2010)

M. J. Tuinier, et al., 2010 had stated in their published paper that there are 3 stages in operating the dynamic bed. The first stage is the cooling stage followed by the capture stage and finally ended with the recovery stage. In each stage, the feed stream to the dynamic bed is different, such as that the feed stream for the first stage is the liquid nitrogen where the bed is cooled down to the cryogenic temperature. The second stage, the mixed gaseous stream of CO<sub>2</sub> and flue gas is fed. In the capture stage, the CO<sub>2</sub> and water is captured in the packed bed. The captured CO<sub>2</sub> and water is recovered in the recovery stage where the pure gaseous CO<sub>2</sub> is fed into the column. The figure 2 shows the mass deposition as well as the axial temperature profile for the cooling stage, capture stage and recovery stage. Detail explanation on the process will be discussed in the next part of this report. The process is a batch process. However, the later work of the same technology makes use of three beds operated in parallel. The cryogenic CO<sub>2</sub> capture using dynamically operated packed bed is the reference technology that is going to be further researched in this project using mixture of carbon dioxide and methane gasses but with the same objective to capture CO<sub>2</sub>.

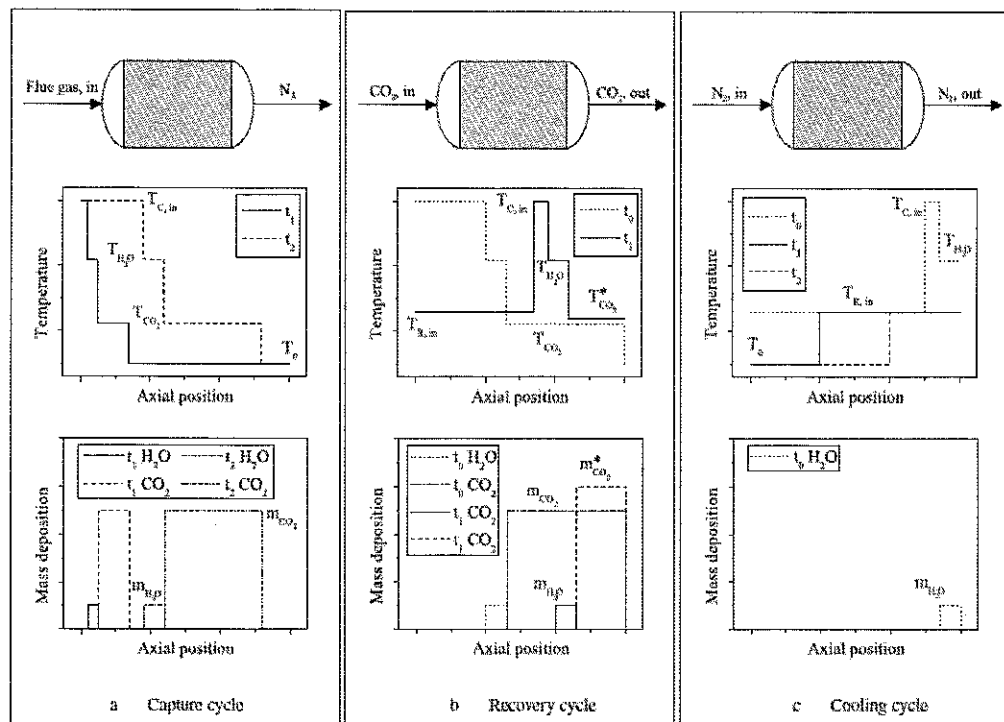


Figure 2: Schematic axial temperature and corresponding mass deposition profiles for the capture (a), recovery (b), and cooling (c) cycle respectively.

However, in the work titled Design Of A Cryogenic CO<sub>2</sub> Capture System Based On Stirling Coolers by Song, et al., 2012a a different approach is taken in capturing the CO<sub>2</sub>. This is because the feed stream is first separated into three flows, namely condensate water, dry ice and residual gas. In the first step, the pre-cool process removes the water from the feed stream by condensing the water through the condensing pipe. This solves the problem of plugging and the rest of the uncondensed gas flow to the freezing tower where CO<sub>2</sub> is desublimated or deposited and scraped to the storage column. The whole process is done at atmospheric pressure. The clean gas exits the system from the gas outlet. The whole process is better described in the figure 3 below:

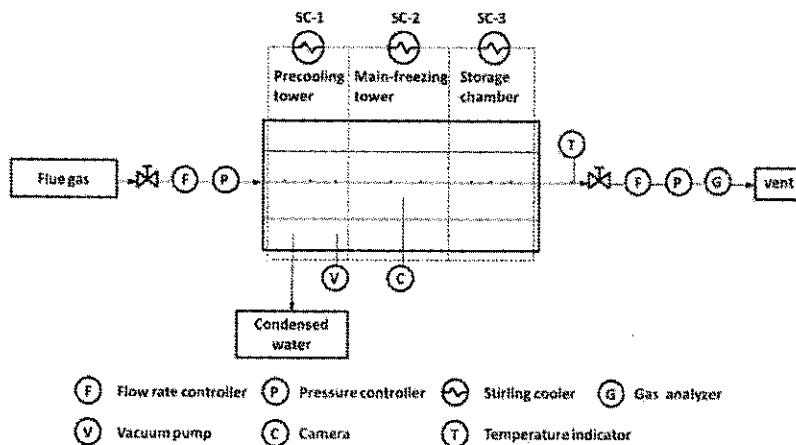


Figure 3: Schematic diagram for cryogenic CO<sub>2</sub> capture system based on stirling coolers

Song, et al., 2012a reported that the problem of plugging is avoided as the CO<sub>2</sub> is captured or deposited onto the heat exchanging surface and scraped by the spinning rod and collected in the storage column where the CO<sub>2</sub> is kept at the cryogenic temperature in the solid form.

Besides that, there are a few of the cryogenic separation technology that has already been applied for commercial application. For example, Ryan Holmes method, Controlled freeze zone (CFZ) method, Cryocell method, Sorex method and Twister technology (Panahi, 2011). As previously mentioned, the cryogenic separation of CO<sub>2</sub> is usually plagued with the problem of plugging by the freezing of substance. Another technology addressing the problem of CO<sub>2</sub> freezing during the cryogenic distillation is the Controlled Freeze Zone or CFZ<sup>TM</sup> developed by the Exxon in the 1980's (Northrop & Valencia, 2009). The column is divided into three operational zones. The top zone is the conventional distillation column while the middle is the controlled freeze zone (CFZ). The bottom of the column is also a conventional distillation column (Panahi, 2011) as in figure 4. The technology key point is to control and confine the CO<sub>2</sub> to a section of the distillation column. The freeze CO<sub>2</sub> will fall into the melt tray while methane will be vaporized. Thus the CO<sub>2</sub> is collected as a liquid. The process is advantageous as all of the sulfur containing compound is collected with the CO<sub>2</sub>. Therefore, higher purity of methane is also possible using this technology. The CFZ technology had already been commercialized by Exxon's at Shute Creek Treatment

Facility in LaBarge, Wyoming (ExxonMobil, 2010) in July 2011 (Panahi, 2011) . According to (ExxonMobil, 2010), the plant that is able to process up to 14 million standard cubic feet per day with the objective to show the ability of the CFZ technology to meet or exceed the specification of sales gas. However, this technology is not suitable for offshore application due to its large footprint.

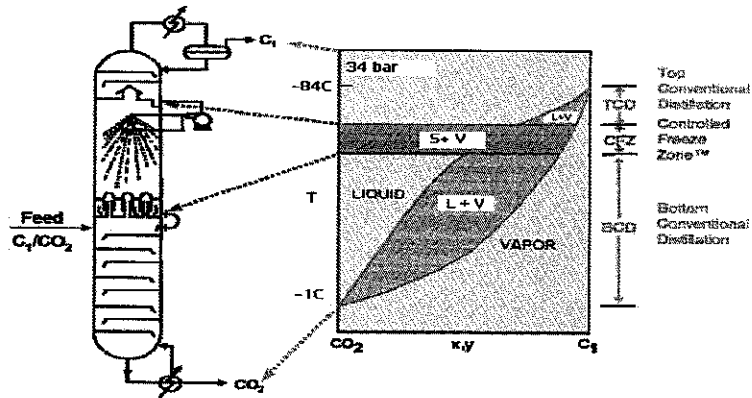


Figure 4: Operational zones of the CFZ technology

Moreover, another commercialized cryogenic separation technology is Ryan Holmes method which is invented by Arthur S. Holmes and James S. Ryan at Koch Process Systems, United States in 1982. The key point of this method is to add solid preventing agents with a freezing temperature below the condenser temperature for example the n-butane (Keskes, et al., 2006) to the solids potential zone of cryogenics distillation column. The addition of the agent will move the liquid composition away from the freezing point. This method is most commonly used in the processing plants.

In addition an emerging technology using the cryogenic separation technology that had already been applied commercially is the Twister technology which is first commercialized in Bintulu, Malaysia in 2004 (Panahi, 2011) for dehydration of sour gas. However, amine absorption process is needed to purify the outlet of twister to the required specifications. Due to its compact size, it is suitable to be applied at offshore platform.

## 2.1.Process Principle

The theory involving cryogenic separation process involves the knowledge on the cryogenics which means temperatures colder than  $-100\text{ }^{\circ}\text{C}$ . The process principle is that the freezing temperature of pure  $\text{CO}_2$  is  $-78.5^{\circ}\text{C}$  at 1atm (Hart & Gnanendran, 2009). Besides that, it is important to know that the freezing temperature of  $\text{CO}_2$  is directly related to the volumetric concentration of  $\text{CO}_2$  in the gas mixture (Clodic, 2002). At the triple point of  $\text{CO}_2$  (5.2atm,  $-56.6^{\circ}\text{C}$ ),  $\text{CO}_2$  will turn into solid phase from the gas phase.  $\text{CO}_2$  melting point is  $-78.5^{\circ}\text{C}$  and boiling point is  $-57^{\circ}\text{C}$  at 1atm. While methane melting point is  $-183^{\circ}\text{C}$  and boiling point is  $-162^{\circ}\text{C}$ . As this project focuses on the separation of water and  $\text{CO}_2$ , it should be noted that the freezing point of water is  $0^{\circ}\text{C}$  and may be lower if there are impurities in the water.

The data for the phase equilibria of  $\text{CO}_2$  – methane system that is crucial in designing the cryogenic separation system can be obtained from various sources. The most commonly known sources is the article published by (Donnelly & Katz, 1954). The article provides extensive data on the equilibria in the  $\text{CO}_2$ – methane system. One of the graph published in the article provide a suitable operating region for this project's proposed cryogenic separation technology of  $\text{CO}_2$  from methane. The graph is represented as in figure 5:

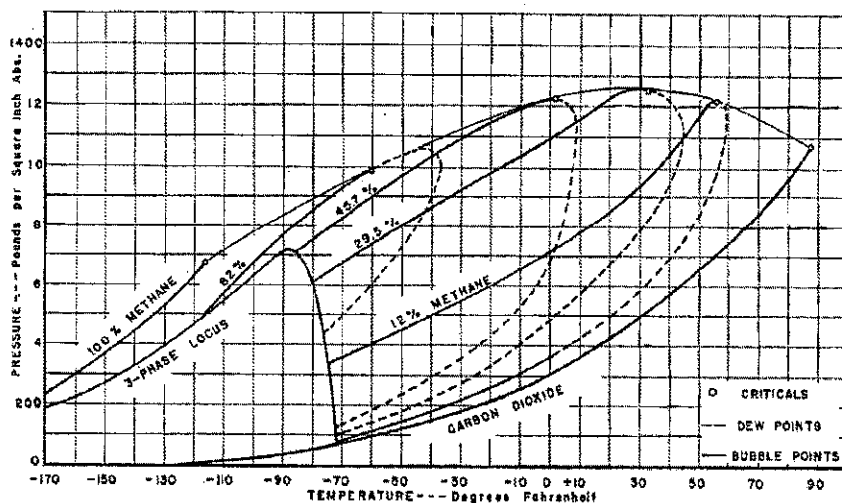


Figure 5: Pressure–temperature relations for carbon dioxide-methane system

Figure 5 shows the “two-phase equilibria for the pure components, three-phase equilibria for the liquid-vapor-solid carbon dioxide and bubble point and dew point line on the vapor and liquid surfaces at designated composition” (Donnelly & Katz, 1954). This graph is a mean to determine the corresponding phase compositions at any temperature and pressure for which vapor and liquid coexist. The constant pressure draft for the same data is shown in figure 6 below where the operating condition of the system is suggested to be in the range of  $-62.2^{\circ}\text{C}$  ( $-80^{\circ}\text{F}$ ) to  $-81^{\circ}\text{C}$  ( $-115^{\circ}\text{F}$ ) for the pressure of 45.78 bar. The temperature range suggested is from the analysis of the graph provided in this report. However, this project will focus on the separation characteristic of methane and carbon dioxide at atmospheric pressure (1 bar), therefore, the optimum working pressure and temperature of the system will be determine with more research and experimentation. This is because as a preliminary research, the hypothesis whether the  $\text{CO}_2$  will be desublimated or deposited onto the packing material is tested first. If this hypothesis works, then more research will be done to optimize this technology.

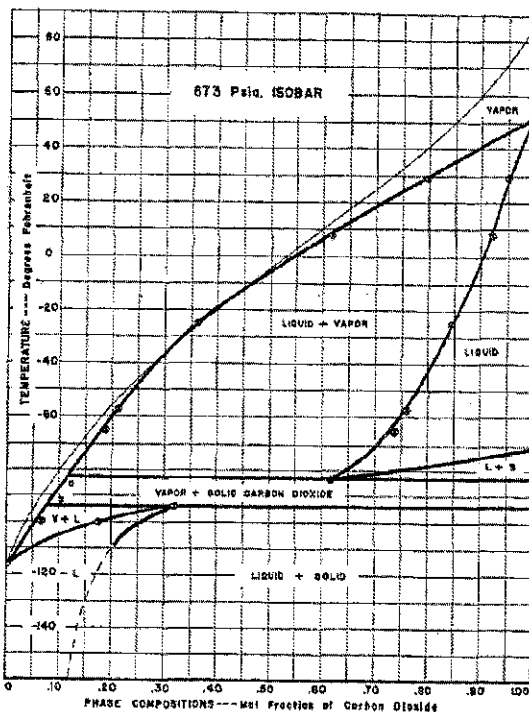


Figure 6: Temperature-composition section system at 673 psia

A phase equilibrium data obtained from ICON simulation is also represented here for the same pressure as the graph in figure 7. The figure 5, figure 6 and figure 7 are good sources in determining the operating condition of the system of the carbon dioxide from methane. However, the analysis from the mathematical modeling and experimentation result will help to verify the data obtain from these sources.

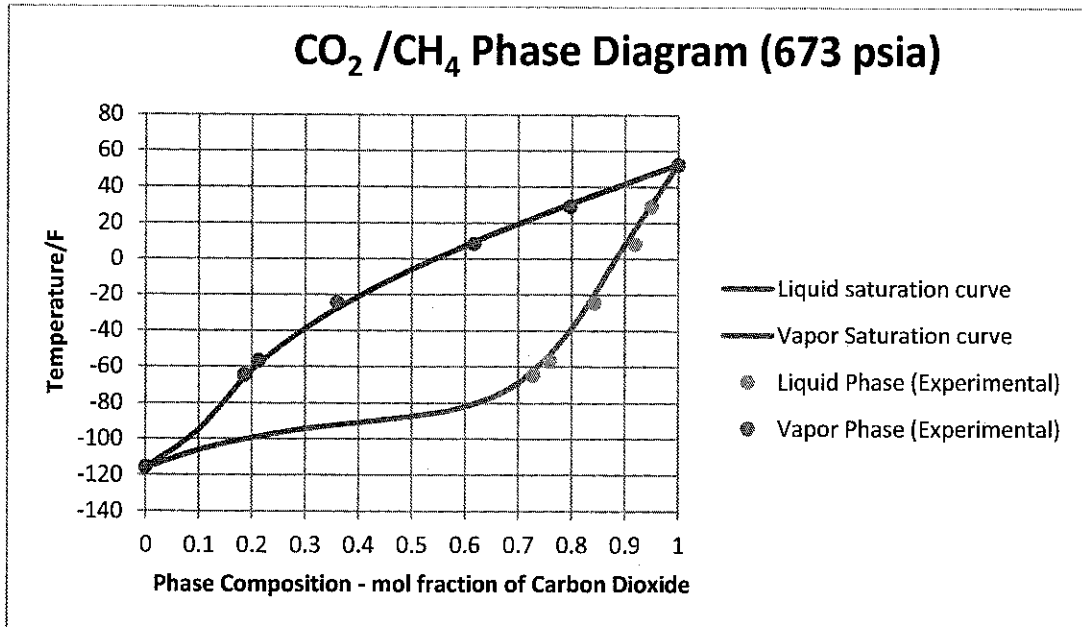


Figure 7: Carbon dioxide – methane system phase diagram for pressure of 673 psia

Referring to the scope and objective of the project, the capture stage is to be explained in this paragraph. In the capture cycles (M. J. Tuinier, et al., 2010), after the packing material is cooled by the liquid nitrogen flow in the cooling cycles. The gas mixture is fed into the system and heat up the packing material as the mixtures is cooled down to a point when the H<sub>2</sub>O is condensed. As condensation takes place, equilibrium temperature is achieved and a condensed front of H<sub>2</sub>O will move toward the end of the bed. However, more hot gas mixture is entering the packed bed at the inlet at the same time, thus the bed is heated from the equilibrium temperature to the inlet temperature. This will create an evaporating front of H<sub>2</sub>O which will move towards the end of the bed. The situation is pictured as a moving condensed front followed by the moving evaporated front of H<sub>2</sub>O. Besides that, the remaining gas mixture is cooled down until the CO<sub>2</sub> starts to de sublimate and a new equilibrium temperature is reached. As the mixtures of gas is

added at the inlet of the packed bed, the fronts of sublimating and de sublimating of CO<sub>2</sub> is created and moving to the outlet of the packed bed. As the CO<sub>2</sub> start to breakthrough, the bed is switched to a regeneration cycle. In regeneration cycle, a pure gaseous CO<sub>2</sub> flow is introduced into the packed bed to recover the frosted CO<sub>2</sub>. At high CO<sub>2</sub> partial pressure, CO<sub>2</sub> loading capacity of the solvent is higher. After all the CO<sub>2</sub> is captured, the bed is switched back to cooling cycles. The simplified description of the process can be viewed as the flue gas is feed into the packed bed, water will be condensed at the hotter region while the CO<sub>2</sub> will be desublimated at the colder region. The bed will be continuously fed with the flue until CO<sub>2</sub> starts to breakthrough and the bed is switched to a recovery stage. In the recovery stage, pure gaseous CO<sub>2</sub> is feed into the bed in order to capture the CO<sub>2</sub> that is desublimated on the packing material. At the end of the recovery stage, water will be left in the bed and it will evaporate and can be flushed out of the bed easily. The whole process is represented in the schematic diagram from figure 8. From the explanation, the concept of the process is consisting of sublimation and desublimation .As stated earlier, sublimation is the phase change from solid gas while desublimation or deposition is the phase change from gas to solid.

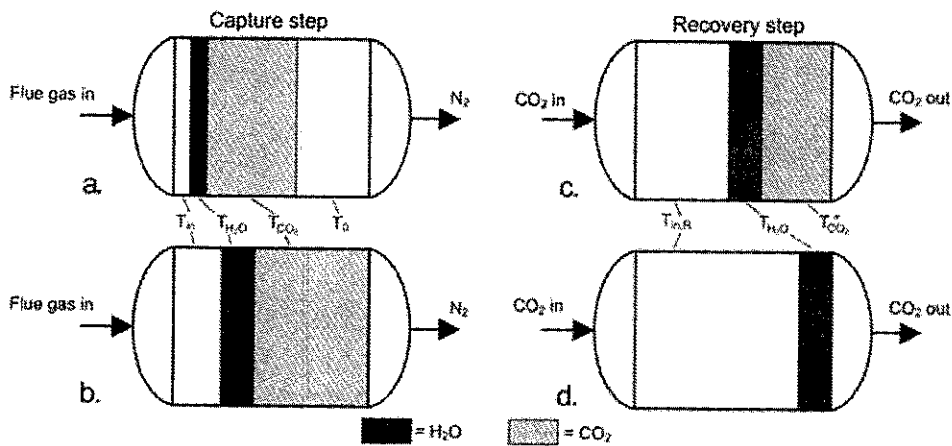


Figure 8: Schematic illustration of the process concept: (a) and (b) during the capture step, (c) and (d) during the recovery step.

The advantage of this process is that the problem of water turned into ice usually encountered in cryogenic separation (S.A. Enbenzer, 2005) is prevented. Therefore, water is not necessarily needed to be completely removed from the gas mixtures.



Moreover, the maximum possible CO<sub>2</sub> capture is achieved if the column is operating at the optimum condition.

## 2.2.Characterization of feed and product

Characterization of feed and product is to be done using the gas chromatograph in order to obtain the standard calibration curve for methane and carbon dioxide. Figure 9 (FONSECA, 2012) show an example of the peaks that can be obtained as a result from gas chromatograph. Available graph on the gas chromatograph calibration data for methane and carbon dioxide is represented in the figure 10 and figure 11 (Stepan, 2009)

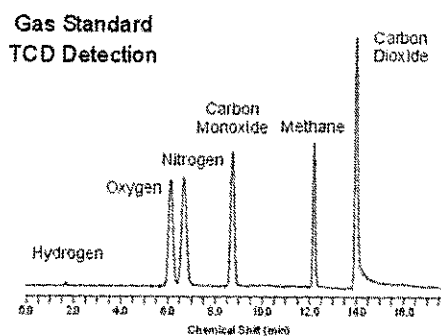


Figure 9: Example of peaks from gas chromatograph

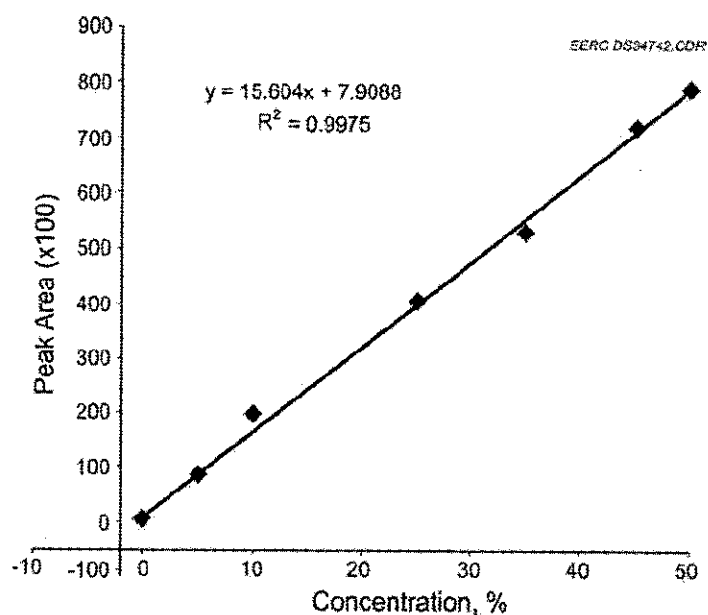


Figure 10: Calibration curve for methane

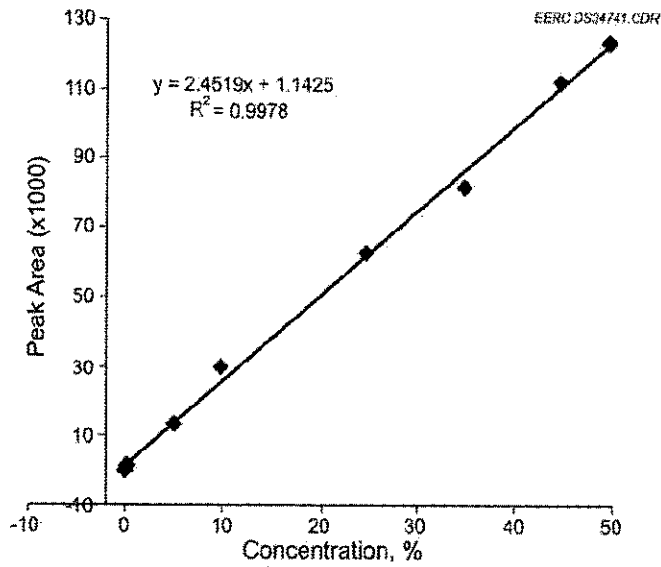


Figure 11: Calibration curve for Carbon Dioxide

These are the example of calibration curve for the carbon dioxide and methane. However, the author is also generating the calibration curve for the sample analysis for experimentation result.

### 2.3. Mathematical Model

The mass transfer processes in the dynamic packed bed is investigated using the 1D plug flow model. The variable associated with the equations is shown in the figure 12:

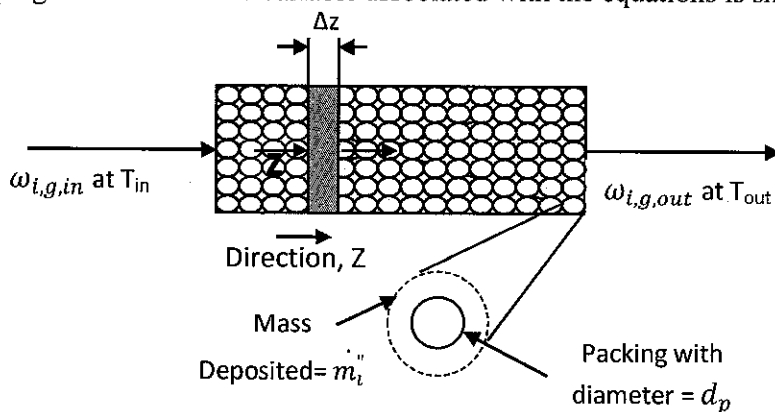


Figure 12: Schematic diagram of packed bed with axial flow.

The model equation is for the one dimensional pseudo-homogenous model which is obtained from M. J. Tuinier, et al., 2010:

Component mass balances for the gas phase:

$$\varepsilon_g \rho_g \frac{\partial \omega_{i,g}}{\partial t} = -\rho_g v_g \frac{\partial \omega_{i,g}}{\partial z} + \frac{\partial}{\partial z} \left( \rho_g D_{eff} \frac{\partial \omega_{i,g}}{\partial z} \right) - \dot{m}_i'' a_s + \omega_{i,g} \sum_{i=1}^{n_c} \dot{m}_i'' a_s$$

Energy balance (gas and solid phase):

$$(\varepsilon_g \rho_g C_{p,g} + \rho_s (1 - \varepsilon_g) C_{p,s}) \frac{\partial T}{\partial t} = -\varepsilon_g \rho_g C_{p,g} \frac{\partial T}{\partial z} + \frac{\partial T}{\partial z} (\lambda_{eff} \frac{\partial T}{\partial z}) - \sum_{i=1}^{n_c} \dot{m}_i'' a_s \Delta h_i$$

Mass deposition rate:

$$\begin{aligned} \dot{m}_i'' &= g(y_{i,s} p - p_i^\sigma) \quad \text{if } y_{i,s} p \geq p_i^\sigma \\ \dot{m}_i'' &= g(y_{i,s} p - p_i^\sigma) \frac{m_i}{m_i + 0.1} \quad \text{if } y_{i,s} p < p_i^\sigma \end{aligned}$$

Where:  $g$  = mass deposition rate constant, s/m

:  $p$  = pressure, Pa

: Gas-solid equilibrium,

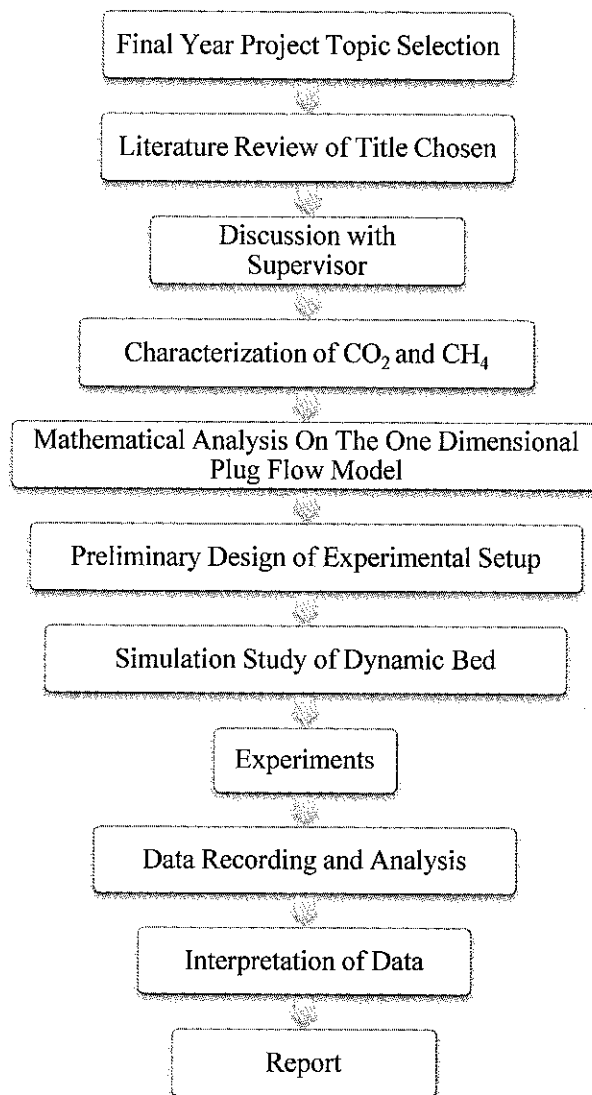
$$p_{CO_2}^\sigma(T) = \exp \left( 10.257 - \frac{3082.7}{T} + 4.08 \ln T - 2.2658 \times 10^{-2} T \right)$$

The model is used to analyze the axial temperature and the mass deposition profiles in the bed. Moreover, the dynamic behavior of the bed may also be described using the one dimensional plug flow model provided above. The details about the terms used in the equation are provided in the nomenclature section. The model will be solved and the result is provided in the result and discussion section.

## CHAPTER 3

### METHODOLOGY

#### 3. RESEARCH METHODOLOGY



### 3.1. Simulations of dynamic packed bed

#### 3.1.1 Assumptions

The mathematical analysis was done based on several assumptions:

- Assuming that the operation is an adiabatic operation and the heat losses to the environment are small. Besides that it is assumed that a uniform velocity profile exists in the absence of radial temperature and concentration gradients. This allows that only the axial temperature and concentration profiles are considered.
- It is assumed that the possible heat transfer limitations between the solid packing and the bulk of the gas phase were accounted for via effective axial heat dispersion (pseudo-homogeneous model).
- It is assumed that mass deposition and sublimation rate of CO<sub>2</sub> is proportional to the local deviation from the phase equilibrium, taking a reasonably short equilibration time constant ( $\tau$ ), which was assumed to be independent of temperature. The rate of sublimation of previously deposited CO<sub>2</sub> was assumed to approach a first order dependency on the mass deposition when this mass deposition approached zero.

The equation is solved by solving each coefficients and acquiring the some properties from the experimental data. Moreover, computer software which is known as Maple is used to generate the curve from the equation after solving for each coefficient.

#### 3.1.2 Model Equations Analysis

The model equation analysis was done based on the properties as in figure 13:

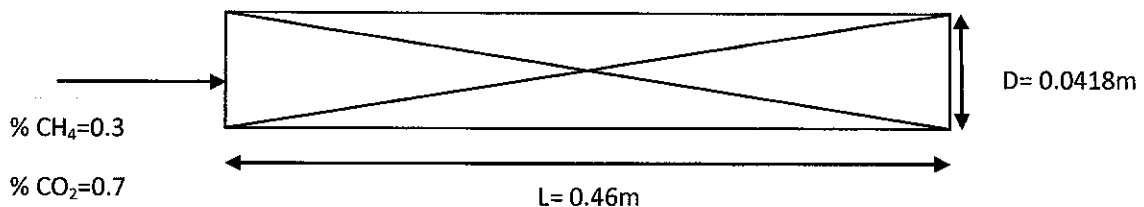


Figure 13: Packed bed properties

With ;  $d_p$  = particle diameter = 0.01 m

Detail solution is shown in the result and discussion part.

### 3.2. Experimental Study on the Cryogenic CO<sub>2</sub> Capture Using Packed Bed.

The experiment is divided into several smaller experiments to obtain certain parameters for the data analysis. The apparatus and equipment needed for the experiment is shown in figure 14, 15,16,17,18 below:

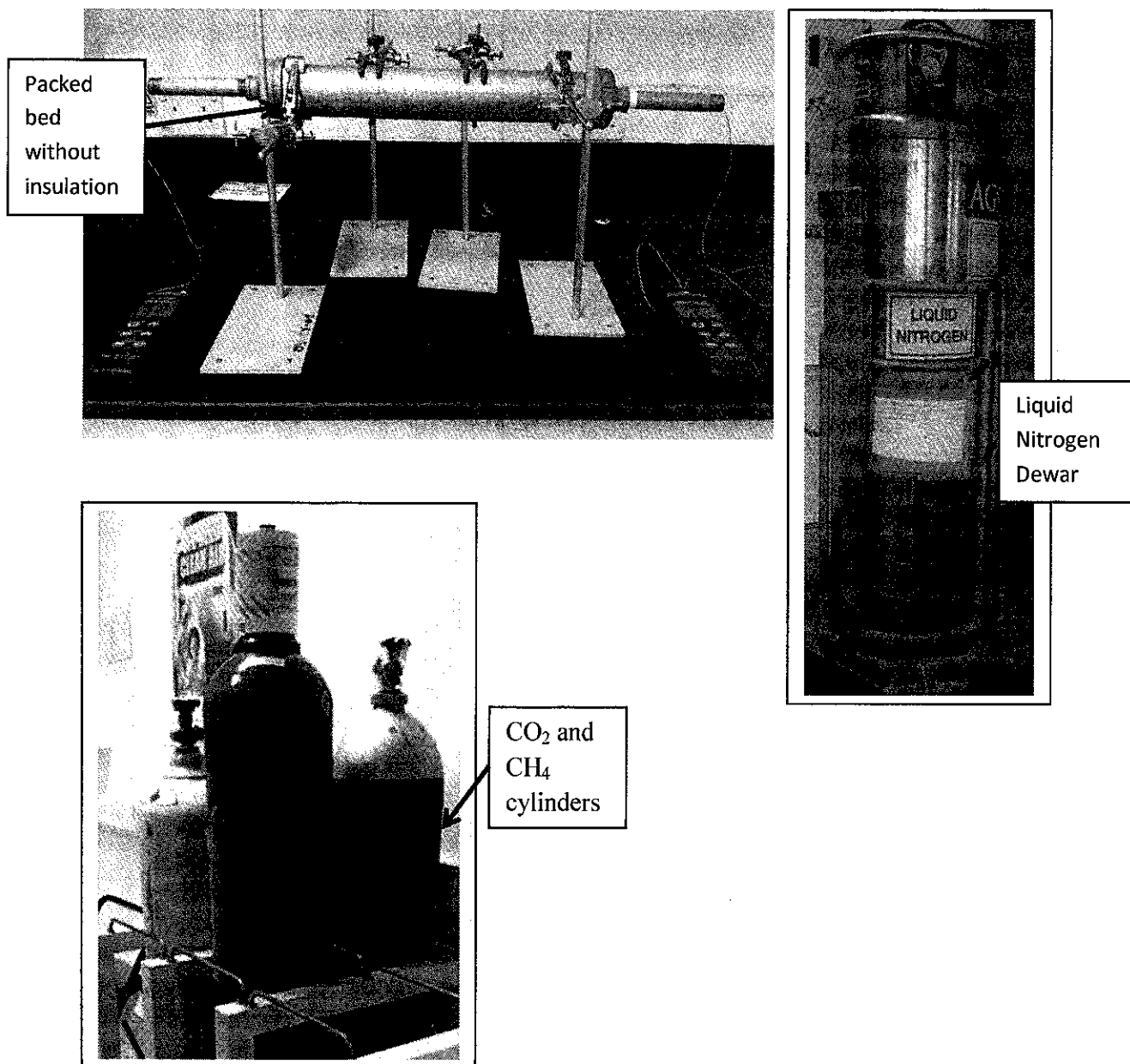


Figure 14: The experimental set up for the cryogenic separation of CO<sub>2</sub> and CH<sub>4</sub> from natural gas with the gas cylinders and the liquid nitrogen Dewar.

The equipment and apparatus shown in figure 14 is connected to the obtain a complete set up of packed bed with the liquid nitrogen Dewar at one end and a CO<sub>2</sub> supply at the other end. As shown in the figure 15.

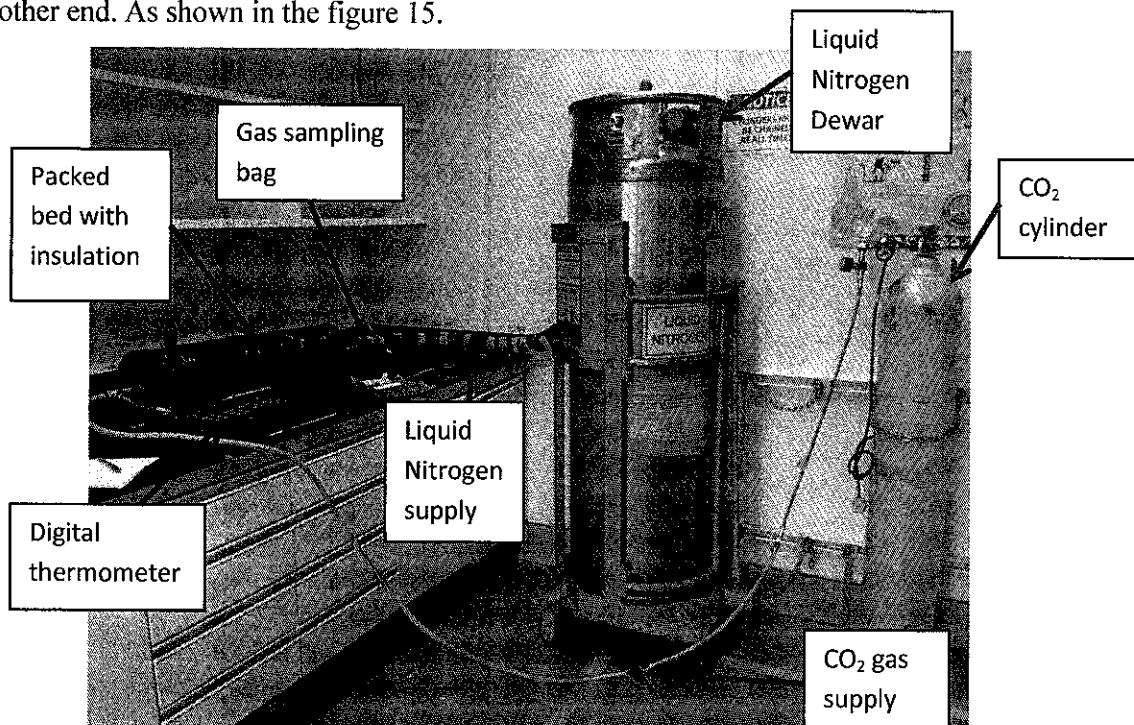


Figure 15: Complete setup of the cryogenic capture of CO<sub>2</sub>

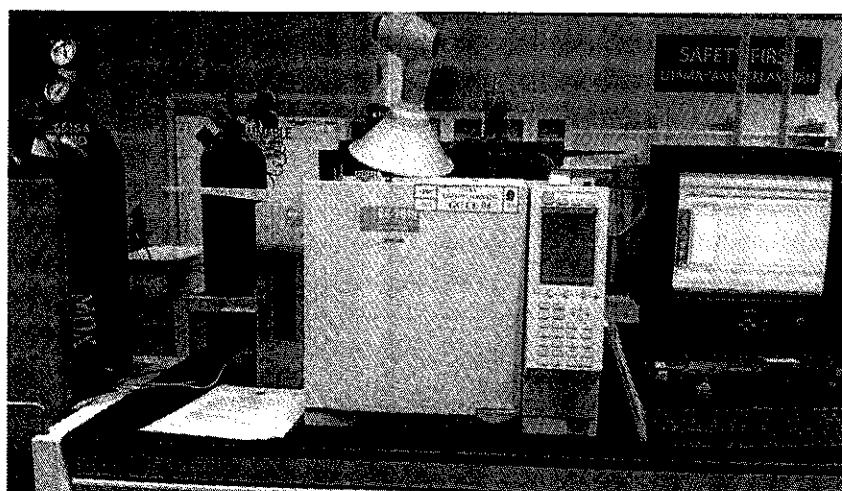


Figure 16: Gas Chromatography Flame Ionization Detector: SHIMADZU GC-20101  
with the item code: GC-CE-04

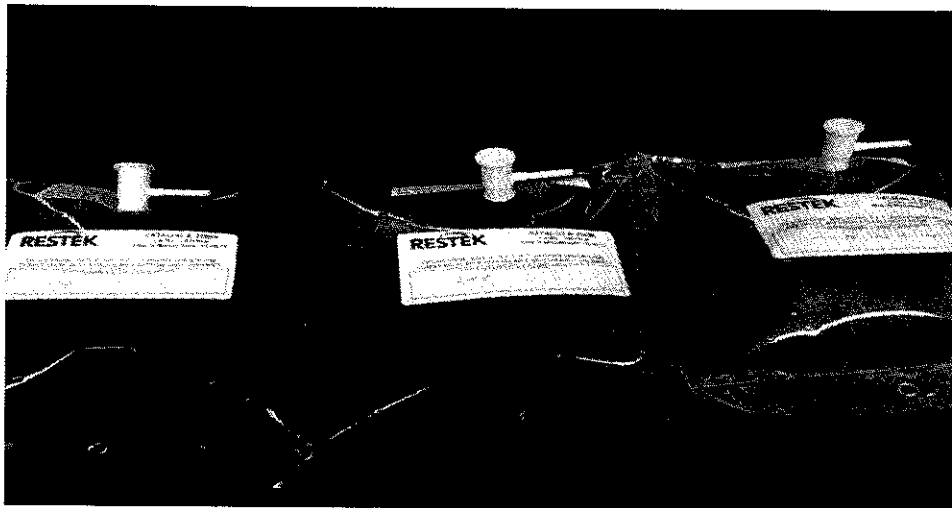


Figure 17: Gas sampling bag containing pure CO<sub>2</sub>, pure CH<sub>4</sub> and a mixture of 60% CO<sub>2</sub> and 40% CH<sub>4</sub>.

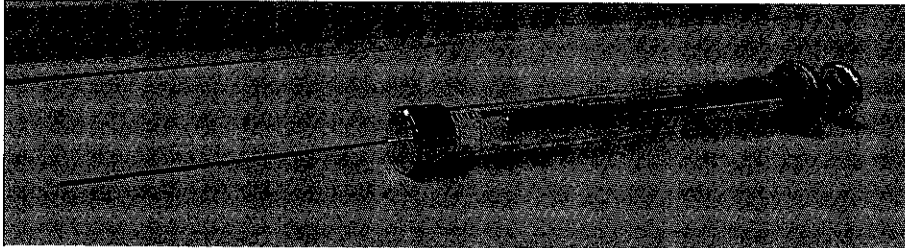


Figure 18: Micro syringe for sample extraction

### 3.2.1. Experiment 1: Calibration Curve for the CO<sub>2</sub> and CH<sub>4</sub> Mixture Using Gas Chromatograph

1. The gas chromatography to be used is the Gas Chromatography Flame Ionization Detector: SHIMADZU GC-20101 with the item code: GC-CE-04.
2. The gas chromatography is turned on and the temperature of the oven is set to be 60°C. 30 minutes is needed to obtain the desired temperature. The other parameter of the gas chromatograph is shown in the appendix.
3. The setting must be the same for every sample that need to be analysed later.
4. The pure CO<sub>2</sub>, pure CH<sub>4</sub> and a known mixture of CO<sub>2</sub> and CH<sub>4</sub> are collected from the gas cylinder into 3 separate gas sampling bag.
5. The septum of each bag is punctured by the micro syringe and 2mm<sup>3</sup> of gases is extracted from the bag and injected into the injection port of gas chromatography.
6. Each of the gas is analysed and a calibration curve is obtained from the analysis.



### **3.1.2 Experiment 2: Obtaining the Void Fraction and Physical Properties of the Bed**

#### **Introduction**

The pipe and marbles that are to be used for the experiment of the cryogenic separation of CO<sub>2</sub> from natural gas must be calibrated to ensure smooth operation later as well as to determine certain parameters that must be known during the experiment.

#### **Objective**

To calibrate the apparatus are to be used for the cryogenic separation of the CO<sub>2</sub> from natural gas and to obtain the dimensions of the apparatus.

#### **Methodology**

1. The apparatus are cleaned using a cleaning powder and wipe dry.
2. The P.V.C tape is applied to the thread of the pipes to ensure no leakage during the experiment.
3. The pipe is connected and the bottom of the pipe is closed using the cap.
4. Stainless steel wool is inserted to the bottom of the pipe. The volume of the pipe occupied by the stainless steel wool is marked at the pipe.
5. Known volume of water is poured into the pipe until it is full. The volume of water,  $V_e$  is recorded as.
6. The water is poured out and the pipe is drained to remove water residue.
7. Marble is inserted into the pipe and finally the stainless steel wool is inserted at the top. The height of the pipe occupied by the marble is marked at the pipe.
8. Known volume of water is poured into the pipe. The volume of water,  $V_m$  with marble is recorded.
9. The experiment is repeated for 5 times.
10. The void fraction of the pipe is calculated.

### **3.1.3 Experiment 3: Obtaining the Heat Transfer Coefficient of the Bed**

#### **Introduction**

Heat transfer across the pipe can be known from experimental procedure. The pipe that are to be used for the experiment of the cryogenic separation of CO<sub>2</sub> from natural gas must be calibrated to ensure smooth operation later as well as to determine certain parameters that must be known during the experiment.

#### **Objective**

To determine the heat transfer coefficient across the pipe for the experiment of the cryogenic separation of CO<sub>2</sub> from natural gas to better understand the heat transfer of the pipe.

#### **Methodology**

1. The packed bed is secured inside a 4" pipe for insulation. This is to create a vacuum space to reduce the heat loss from the packed bed.
2. The temperature probes is secured in position.
3. The 4" pipe is wrapped in the rubber insulation called Hypalon for safety purposes as well as to minimise heat loss from the packed bed.
4. Tubing is connected from the liquid nitrogen Dewar to the end of the packed bed.
5. The valve at the liquid nitrogen Dewar is open slowly and liquid nitrogen is supplied into the packed bed.
6. After the temperature of the packed bed reaches -50°C, the liquid nitrogen supply is stopped and the stop watch is started.
7. The temperature of the packed bed is taken every 10 seconds for 1 minute and every 1 minute after the first minute.
8. The temperature is recorded and analysed.

### 3.1.4 Experiment 4: Cryogenic CO<sub>2</sub> Capture

Figure 20 shows the schematic diagram for the setup of the main experiment.

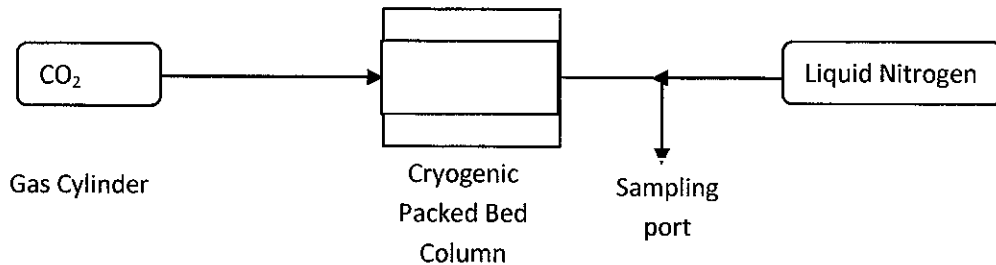


Figure 19: Experimental setup of cryogenic CO<sub>2</sub> separation

Due to the time constraint as well as lack of suitable equipment, the experiment is done at the atmospheric pressure.

The procedure of the experiment is as follows:

- The equipment, cylinder and liquid nitrogen Dewar is connected using suitable fittings as in the figure 19.
- The dynamic packed bed column temperature is cooled down to the cryogenic temperature with the range of (-80 °C to -100 °C) using a liquid nitrogen supply system.
- The flow of the liquid nitrogen is stopped after it reaches -110 °C and the CO<sub>2</sub> is supplied to the packed bed.
- Temperature along the bed is taken for every 3 minutes.
- The temperature profile along the bed is observed.
- The sample is collected at the end of the column to be analysed using the gas chromatograph (GC).

The variables for the experiment to be noted are:

- Temperature profile.
- Velocity of the moving front computed from experiment data.
- Concentration of the outlet stream at inlet and outlet and at  $T_{in}$  and  $T_{out}$

### 3.2 Gantt Chart

#### 3.2.2 Gantt Chart for Final Year Project 1

| No. | Detail/Week  | 1 | 2 | 3 | 4 | 5 | 6 | 7 | 8 | 9 | 10 | 11 | 12 | 13 | 14 |
|-----|--|---|---|---|---|---|---|---|---|---|----|----|----|----|----|
| 1   | Selection of Project Title                           |   |   |   |   |   |   |   |   |   |    |    |    |    |    |
| 2   | Literature Search of Study                           |   |   |   |   |   |   |   |   |   |    |    |    |    |    |
| 3   | Process Flow Diagram for Experimental Study          |   |   |   |   |   |   |   |   |   |    |    |    |    |    |
|     | Develop Methodology for Experiment                   |   |   |   |   |   |   |   |   |   |    |    |    |    |    |
|     | Preliminary Simulation Study                         |   |   |   |   |   |   |   |   |   |    |    |    |    |    |
| 4   | Submission of Extended Proposal Defence (Max 5 Page) |   |   |   |   |   |   |   |   |   |    |    |    |    |    |
| 5   | Proposal Defence                                     |   |   |   |   |   |   |   |   |   |    |    |    |    |    |
| 6   | Project Work   |   |   |   |   |   |   |   |   |   |    |    |    |    |    |
|     | Simulation Study of Separation Characteristics       |   |   |   |   |   |   |   |   |   |    |    |    |    |    |
|     | Preliminary Design of Experimental Setup             |   |   |   |   |   |   |   |   |   |    |    |    |    |    |
|     | Simulation Study of Dynamic Bed                      |   |   |   |   |   |   |   |   |   |    |    |    |    |    |
|     | Characterization of Feed and Products                |   |   |   |   |   |   |   |   |   |    |    |    |    |    |
| 7   | Prepare the Interim Draft Report                     |   |   |   |   |   |   |   |   |   |    |    |    |    |    |
| 8   | Submission of Interim Draft Report                   |   |   |   |   |   |   |   |   |   |    |    |    |    |    |
| 9   | Submission of Interim Report (Max 25 Page)           |   |   |   |   |   |   |   |   |   |    |    |    |    |    |

Mid-Semester Break

3.2.3 Gantt Chart for Final Year Project 2

| No. | Detail/Week                                     | 1 | 2 | 3 | 4 | 5 | 6 | 7 | Mid-Semester Break |  |  |  |  |  |  | 13 | 14 | 15 |
|-----|---|---|---|---|---|---|---|---|--------------------|--|--|--|--|--|--|----|----|----|
| 1   | Project Work Continues                          |   |   |   |   |   |   |   |                    |  |  |  |  |  |  |    |    |    |
| 2   | Submission of Progress Report                   |   |   |   |   |   |   |   |                    |  |  |  |  |  |  |    |    |    |
| 3   | Project Work Continues                          |   |   |   |   |   |   |   |                    |  |  |  |  |  |  |    |    |    |
| 4   | Pre-SEDEX                                       |   |   |   |   |   |   |   |                    |  |  |  |  |  |  |    |    |    |
| 5   | Submission of Draft Report to SV to check       |   |   |   |   |   |   |   |                    |  |  |  |  |  |  |    |    |    |
| 6   | Submission of Dissertation (soft bound)         |   |   |   |   |   |   |   |                    |  |  |  |  |  |  |    |    |    |
| 7   | Submission of Technical Paper to SV             |   |   |   |   |   |   |   |                    |  |  |  |  |  |  |    |    |    |
| 7   | Oral Presentation                               |   |   |   |   |   |   |   |                    |  |  |  |  |  |  |    |    |    |
| 8   | Submission of Project Dissertation (Hard Bound) |   |   |   |   |   |   |   |                    |  |  |  |  |  |  |    |    |    |

## CHAPTER 4

### RESULT AND DISCUSSION

#### 4 RESULT AND DISCUSSION

##### 4.1 Simulations of dynamic packed bed

##### 4.1.2 Analysis of Model Equation for Component Mass Balance and ( Simulation of Dynamic Packed Bed)

To describe the mass deposition rate with respect to temperature as well as the component mass balance and the energy balance for the process, mathematical analysis was carried out. The analysis on the model equation was done based on these bases:

100 liter of CO<sub>2</sub> and CH<sub>4</sub> mixture of 70% CO<sub>2</sub> and 30% CH<sub>4</sub>.

100 liter mixture contain 70 liter CO<sub>2</sub>

$$\text{mass of CO}_2 = \frac{70}{22.4} \text{ moles} = 3.125 \text{ moles} = 137.5g$$

100 liter mixture contain 30 liter CH<sub>4</sub>

$$\text{mass of CH}_4 = \frac{30}{22.4} \text{ moles} = 1.34 \text{ moles} = 21.4g$$

$$\text{Total mass of gas mixture} = 21.4 + 137.5 = 158.9 g$$

**Conditions and quantities used in numerical studies:**

Table 1: Conditions and coefficients values used in the numerical studies

| Conditions or Coefficients  | Values                                    |
|---|---|
| Temperature of gas mixture [T]  | 25°C                                      |
| Pressure of gas mixture [P]   | 1.01325 bar                               |
| Flow rate of gas mixture [q]  | 1.82 x 10 <sup>-4</sup> m <sup>3</sup> /s |
| Diameter of bed [D]   | 0.0418 m                                  |
| Diameter of particle [d <sub>p</sub> ]  | 0.01 m                                    |
| Density of particle [ρ <sub>s</sub> ]   | 2562 kg/m <sup>3</sup>                    |
| Density of gas mixture (CO <sub>2</sub> & CH <sub>4</sub> ) [ρ <sub>g</sub> ]                             | 1.46 kg/m <sup>3</sup>                    |
| Superficial velocity [v <sub>g</sub> ]  | 0.133 m/s                                 |
| Bed void fraction [ε <sub>g</sub> ]   | 0.637                                     |
| Viscosity [μ]   | 0.00001114 NS/m <sup>2</sup>              |
| Effective bed conductivity [λ <sub>bed,0</sub> ]  | 1 w/mk                                    |
| Heat capacity of CH <sub>4</sub> and CO <sub>2</sub> mixture [C <sub>p,g</sub> ]                          | 0.036 J/kgK                               |
| Mixture thermal conductivity [λ <sub>g</sub> ]  | 0.0172 w/mk                               |
| Enthalpy change related to phase change of CO <sub>2</sub> [Δh <sub>CO<sub>2</sub></sub> <sup>sub</sup> ] | 5.682x10 <sup>5</sup> J/kg                |

**Component mass balance for the gas phase:**

$$\varepsilon_g \rho_g \frac{\partial \omega_{i,g}}{\partial t} = -\rho_g v_g \frac{\partial \omega_{i,g}}{\partial z} + \frac{\partial}{\partial z} \left( \rho_g D_{eff} \frac{\partial \omega_{i,g}}{\partial z} \right) - \dot{m}_i'' a_s + \omega_{i,g} \sum_{i=1}^{n_c} \dot{m}_i'' a_s \quad (1)$$

Solving for each coefficient in the mass and energy balance equation:

**Volume of bed, V<sub>Bed</sub>:**

$$V_{Bed} = \pi r^2 h = \pi \times 0.0209^2 \times 0.46 \text{ m} = 6.312 \times 10^{-4} \text{ m}^3$$

**Density of gas, ρ<sub>g</sub>:**

Volume of gas, V<sub>1</sub>

$$\frac{P_1 V_1}{T_1} = \frac{P_2 V_2}{T_2}$$

$$\frac{1 * V_1}{298 \text{ K}} = \frac{1 * 100 \text{ l}}{273 \text{ K}}$$

$$V_1 = 109.16 \text{ l}$$

$$\text{Density, } \rho_g = \frac{\text{mass}}{\text{volume}}$$

$$\text{Density, } \rho_g = \frac{158.9 \text{ g}}{109.16 \text{ l}} = 1.46 \frac{\text{g}}{\text{l}} = 1.46 \frac{\text{kg}}{\text{m}^3}$$

**Superficial velocity,  $v_g$ :**

$$v_g = \frac{\text{Volumetric flow rate of gas}}{\text{Cross sectional area}} = Q/A$$

$$v_g = \frac{1.82 \times 10^{-4} \frac{\text{m}^3}{\text{s}}}{\pi \cdot (0.0209)^2} = 0.133 \text{ m/s}$$

**Effective diffusion coefficient,  $D_{eff}$ :**

$$D_{eff} = v_g d_p \left( \frac{0.73}{ReSc} + \frac{0.5}{\varepsilon_g \left( 1 + \frac{9.7 \varepsilon_g}{ReSc} \right)} \right)$$

*Calculating for Reynolds number,  $Re$ :*

$$Re = \frac{\rho_g v_g d_p}{\mu}$$

From the equation for Reynolds number calculations, we need to know the gas mixture viscosity. The Herning & Zipperer equation is used to calculate the gas mixture viscosity:

$$\mu = \frac{\sum_i^n r_i \mu_i \sqrt{M_i T_{ci}}}{\sum_i^n r_i \sqrt{M_i T_{ci}}}$$

*Where:*

$r_i$  = volume ratio of component  $i$ ,  $r_{CO_2} = 70$  and  $r_{CH_4} = 30$

$\mu_i$  = Absolute or dynamic viscosity of component  $i$ ,

$\mu_{CO_2} = 0.0001493$  poise and  $\mu_{CH_4} = 0.0001114$  poise



$M_i$  = Molar mass of component  $i$ ,  $M_{CO_2} = 44$  and  $M_{CH_4} = 16$

$T_{ci}$  = Critical temperature of component  $i$ ,  $T_{CO_2} = 304$  K and  $T_{CH_4} = 190.3$  K

Now putting the values into the Hering & Zipperer equation:

$$\mu = \frac{70 \times 0.0001493 \times \sqrt{44 \times 304} + 30 \times 0.0001114 \times \sqrt{(16 \times 190.3)}}{70 \times \sqrt{44 \times 304} + 30 \times \sqrt{(16 \times 190.3)}}$$

$$\mu = 0.0001114 \text{ poise} = 0.00001114 \frac{N \cdot s}{m^2}$$

Now putting all known values in Reynolds number equation:

$$Re = \frac{1.46 \times 0.133 \times 0.01}{0.0000144} = 134.85$$

Schmidt Number,  $Sc$ , is a dimensionless parameter representing the ratio of diffusion of momentum to the diffusion of mass in a fluid. For gases,  $Sc \approx 0.7$

Putting all the values into the diffusion coefficient equation to obtain  $D_{eff}$ :

$$D_{eff} = 0.133 \text{ m/s} \times 0.01 \text{ m} \left( \frac{0.73}{134.85 \times 0.7} + \frac{0.5}{0.637 \left( 1 + \frac{9.7 \times 0.637}{134.85 \times 0.7} \right)} \right)$$

$$D_{eff} = 0.000987321 \frac{m^2}{s}$$

**Specific solid surface area per unit bed volume,  $a_s$ :**

$$a_s = \frac{6}{d_p} (1 - \varepsilon_g)$$

$$a_s = \frac{6}{0.01 \text{ m}} (1 - 0.637) = 217.8 \frac{m^2}{m^3}$$

**Mass Deposition Rate,  $\dot{m}_i$ :**

$$\dot{m}_i = g(y_{i,s}P - p_i^\sigma) \text{ if } y_{i,s}P \geq p_i^\sigma$$

$$\dot{m}_i = g(y_{i,s}P - p_i^\sigma) \frac{m_i}{m_i + 0.1} \text{ if } y_{i,s}P < p_i^\sigma$$

Where:  $g$  = mass deposition rate constant,  $s/m = 1.0e-06$  s/m

:  $P = \text{pressure, Pa} = 101.3\text{kPa}$

: Gas-solid equilibrium,

$$p_{CO_2}^{\sigma}(T) = \exp\left(10.257 - \frac{3082.7}{T} + 4.08 \ln T - 2.2658 \times 10^{-2} T\right)$$

Mass deposition rate was calculated for different concentration of  $CO_2$  at different temperature and is shown in the table 2 below:

Table 2: Mass deposition rate at different temperature for different  $CO_2$  concentration:

|      |        | $Y_{CO_2}$             |                |                |                |                |                |                |                |                |                |
|------|--------|------------------------|----------------|----------------|----------------|----------------|----------------|----------------|----------------|----------------|----------------|
|      |        | $Y_{CO_2}$             | $Y_{CO_2}$     | $Y_{CO_2}$     | $Y_{CO_2}$     | $Y_{CO_2}$     | $Y_{CO_2}$     | $Y_{CO_2}$     | $Y_{CO_2}$     | $Y_{CO_2}$     | $Y_{CO_2}$     |
|      |        | 0.2                    | 0.3            | 0.4            | 0.5            | 0.6            | 0.7            | 0.8            | 0.9            | 1              |                |
| T(C) | T(K)   | $p_{CO_2}^{\sigma}(T)$ | $m_i^{\prime}$ | $m_i^{\prime}$ | $m_i^{\prime}$ | $m_i^{\prime}$ | $m_i^{\prime}$ | $m_i^{\prime}$ | $m_i^{\prime}$ | $m_i^{\prime}$ | $m_i^{\prime}$ |
| -50  | 223.15 | 694117.85              | -              | -              | -              | -              | -              | -              | -              | -              | -              |
| -60  | 213.15 | 377681.50              | -              | -              | -              | -              | -              | -              | -              | -              | -              |
| -70  | 203.15 | 191074.71              | -              | -              | -              | -              | -              | -              | -              | -              | -              |
| -80  | 193.15 | 88913.42               | -              | -              | -              | -              | -              | -              | 0.00           | 0.01           | -              |
| -90  | 183.15 | 37559.25               | -              | -              | 0.00           | 0.01           | 0.02           | 0.03           | 0.04           | 0.05           | 0.06           |
| -100 | 173.15 | 14173.01               | 0.01           | 0.02           | 0.03           | 0.04           | 0.05           | 0.06           | 0.07           | 0.08           | 0.09           |
| -110 | 163.15 | 4683.12                | 0.02           | 0.03           | 0.04           | 0.05           | 0.06           | 0.07           | 0.08           | 0.09           | 0.10           |
| -120 | 153.15 | 1321.44                | 0.02           | 0.03           | 0.04           | 0.05           | 0.06           | 0.07           | 0.08           | 0.09           | 0.10           |
| -130 | 143.15 | 308.41                 | 0.02           | 0.03           | 0.04           | 0.05           | 0.06           | 0.07           | 0.08           | 0.09           | 0.10           |
| -140 | 133.15 | 57.12                  | 0.02           | 0.03           | 0.04           | 0.05           | 0.06           | 0.07           | 0.08           | 0.09           | 0.10           |
| -150 | 123.15 | 7.95                   | 0.02           | 0.03           | 0.04           | 0.05           | 0.06           | 0.07           | 0.08           | 0.09           | 0.10           |
| -160 | 113.15 | 0.77                   | 0.02           | 0.03           | 0.04           | 0.05           | 0.06           | 0.07           | 0.08           | 0.09           | 0.10           |
| -170 | 103.15 | 0.05                   | 0.02           | 0.03           | 0.04           | 0.05           | 0.06           | 0.07           | 0.08           | 0.09           | 0.10           |

From the data in the table 2, mass deposition rate for 70 %  $CO_2$  and 30 %  $CH_4$  at  $-140^{\circ}C$ ,

$$m_i^{\prime} = 0.7$$

**Peclet number for axial heat dispersion,  $Pe_{ax}$**

$$Pe_{ax} = \frac{2p}{1-p}, \quad P_a = 0.17 + 0.33 \exp \frac{-24}{Re}$$

$$P_a = 0.17 + 0.33 \exp \frac{-24}{134.85} = 0.4462$$

$$Pe_{ax} = \frac{2(0.4462)}{1 - 0.4462} = 1.6114$$

**Prandtl number, Pr:**

$$Pr = \frac{Cp_g \mu}{\lambda_g} = \frac{2.188 \times 0.0000144}{0.0172} = 0.00183$$

**Gas to particle heat transfer coefficient, Nu:**

$$Nu = \left(7 - 10\varepsilon_g + 5\varepsilon_g^2\right)(1 + 0.7 Re^{0.2} Pr^{\frac{1}{3}}) + (1.33 - 2.4\varepsilon_g + 1.2 \varepsilon_g^2) Re^{0.7} Pr^{\frac{1}{3}}$$

$$Nu = \left((7 - 10(0.637) + 5(0.637)^2)(1 + 0.7 (0.637)^{0.2} (0.00183)^{\frac{1}{3}})\right) + (1.33 - 2.4(0.637) + 1.2 (0.637)^{0.2})0.637^{0.7}(0.00183)^{\frac{1}{3}}$$

$$Nu = 2.6673$$

**Effective axial heat dispersion in a transient packed bed (Vortmeyer and Berninger, 1982),  $\lambda_{eff}$ :**

$$\lambda_{eff} = \lambda_{bed,0} + \frac{RePr\lambda_g}{Pe_{ax}} + \frac{Re^2Pr^2\lambda_g}{6(1 - \varepsilon_g)Nu}$$

$$\lambda_{eff} = 1 \text{ w/mk} + \frac{134.85 \times 0.00183 \times 0.0172}{1.6114} + \frac{134.85^2 \times 0.00183^2 \times 0.0172}{6(1 - 0.637)2.6673}$$

**Thus, component mass balance for the gas phase:**

Putting the calculated coefficient for the component mass balance for the gas phase and we will get this equation which is solved using computer software.

*Component mass balance for the gas phase becomes:*

$$0.93002 \frac{\partial \omega_{i,g}}{\partial t} = -0.19418 \frac{\partial \omega_{i,g}}{\partial z} + 1.44e - 3 \left( \frac{\partial^2 \omega_{i,g}}{\partial z^2} \right) - 26.2514$$

*Energy balance for gas and solid phase becomes:*

$$(630.7) \frac{\partial T}{\partial t} = -0.0098 \frac{\partial T}{\partial t} + \frac{\partial}{\partial t} \left( 3.7 \frac{\partial^2 T}{\partial z^2} \right) - 333.6$$

The curve obtained for the mathematical analysis is presented in figure 20 and figure 21.

For the internal boundary boundary condition for component mass balance:

At:  $z = 0, \omega_{CO_2,g} = 70$

$t = 0, \omega_{CO_2,g} = 70$

Assuming all of  $CO_2$  is captured;

At:  $z = 1, \omega_{CO_2,g} = 0$

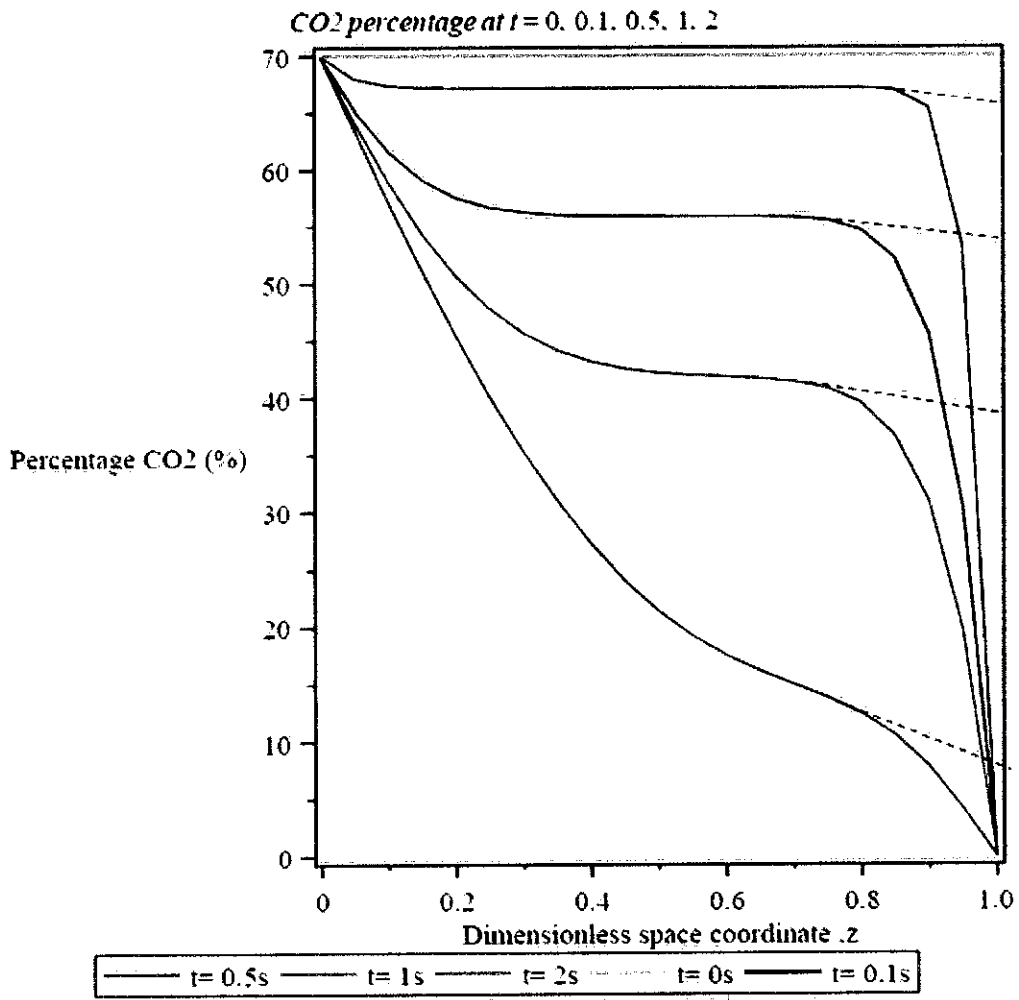


Figure 20: The curve generated for the change in percentage of  $CO_2$  in the  $z$  direction for the different time.

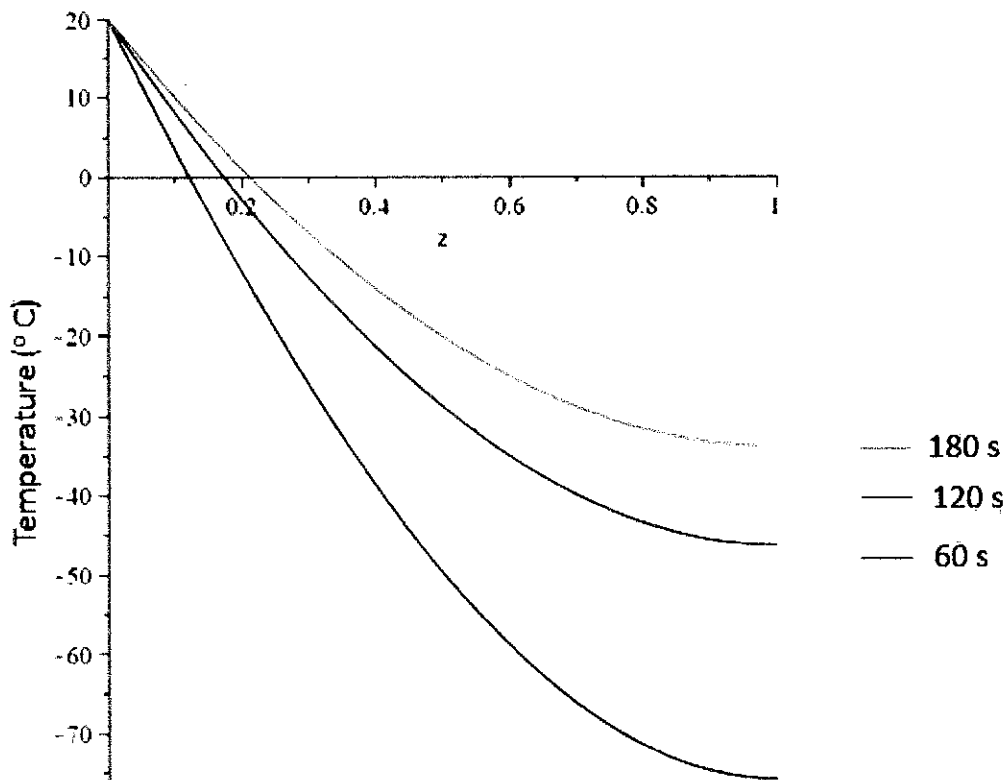


Figure 21: The curve generated from energy balance for change in temperature of packed bed in the  $z$  direction for different time.

The graph in figure 20 shows the different mass fraction of  $\text{CO}_2$  for different time ( $t$ ) at different location ( $z$ ). From the graph, we can see that there is no deposition of  $\text{CO}_2$  at any location in the bed at time 0 minutes. This is shown by the straight line which is representing the same fraction of the  $\text{CO}_2$  as in the inlet. This is because the  $\text{CO}_2$  flow has just been introduced into the packed bed. However, as the time increase, we can see that there are more  $\text{CO}_2$  deposited in the packed bed. The dotted line in the graph represent the mass fraction of  $\text{CO}_2$  is the boundary condition is not set for only until  $z = 1$ . The dotted line is can be studied experimentally.

The graph in figure 21 shows the change in temperature of packed bed in the  $z$  direction for different time. The graph shows that for shorter time the feed gas spent in the packed bed, the smaller the change in the temperature of the packed bed. This is due to shorter time for the feed gas to contact with the packing material for heat transfer to occur.

Finally at time 2 minutes, the mass fraction of CO<sub>2</sub> in the gas mixture is 0. This means that all CO<sub>2</sub> is deposited in the packed bed. However, this is the solution that is obtained from simulation results.

#### 4.1.3 Analysis of the Mass Deposition Rate

The mass deposition rate was calculated and the result obtained is shown in the table 2. A mass deposition rate versus temperature graph was generated in figure 22:

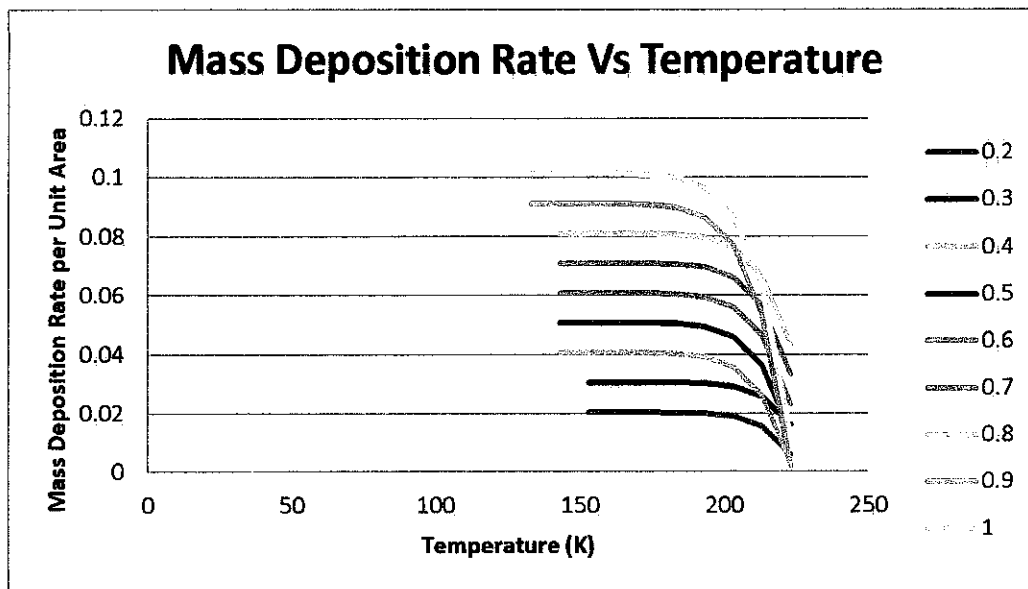


Figure 22: Mass deposition rate versus temperature

#### Discussion

The curve obtained for different concentration of CO<sub>2</sub> shows the mass deposition rate for the higher concentration of CO<sub>2</sub> is higher. This shows a potential that the cryogenic separation using the dynamic packed bed is suitable for separation of high concentration of CO<sub>2</sub> from the natural gas. Moreover, as the concentration of CO<sub>2</sub> increases, the slope is steeper, thus slight temperature change will affect the mass deposition rate. Therefore, it is important to make use of this and work on the small temperature range in order to find the optimum working temperature rather than to work on the broader temperature range which will be more time consuming.

Besides that, the amount of CO<sub>2</sub> deposited increases as the temperature decreases. However, for temperature 163.15 K (-110°C) and above, the deposition rate is almost constant. Therefore, it is decided to perform the experiment in the range of 193.15 K (80°C) to 163.15 K (110°C). This is because, the CO<sub>2</sub> started to be deposited at the temperature of 80°C.

#### 4.1.4 Experimental Study On The Cryogenic CO<sub>2</sub> Capture Using Packed Bed

Data gathered from experiment:

##### *Experiment 1: Calibration Curve for the CO<sub>2</sub> and CH<sub>4</sub> Mixture Using Gas Chromatograph*

The results for experiment 1 is shown in the appendix titled, result of Experiment 3: Obtaining the Calibration Curve for the CO<sub>2</sub> and CH<sub>4</sub> Mixture Using Gas Chromatograph. One of the curves generated from GC is shown in figure 23.

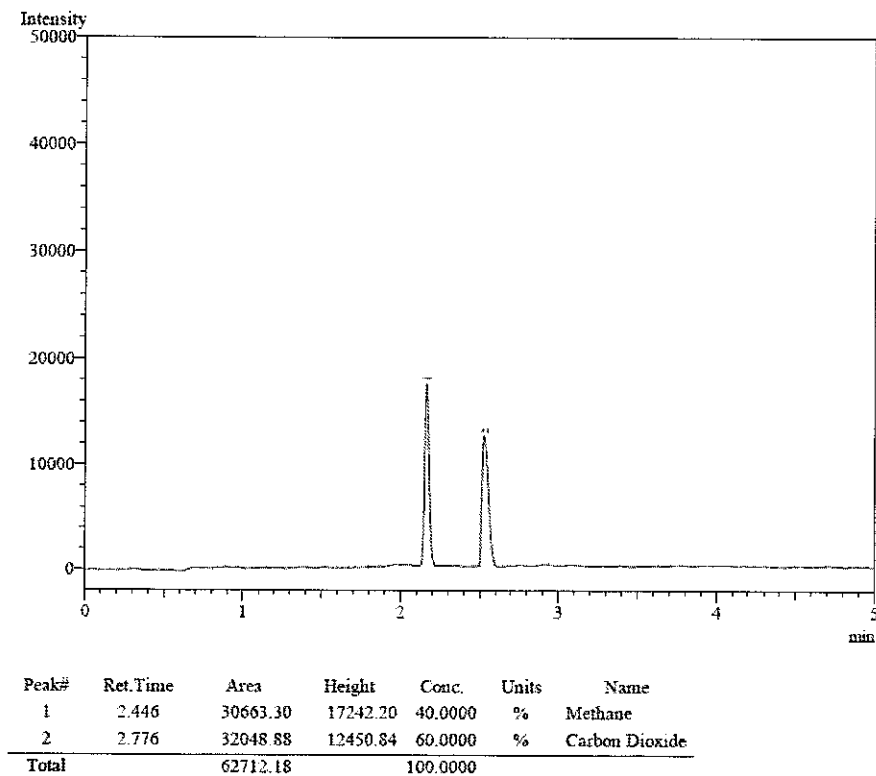


Figure 23: Result from a known sample analysis using gas chromatograph

The data obtained from GC for various concentrations of CO<sub>2</sub> and CH<sub>4</sub> is used to generate the calibration curve for the quantitative analysis of gas mixture sample. The calibration curves obtained are shown in figure 24 and 25:

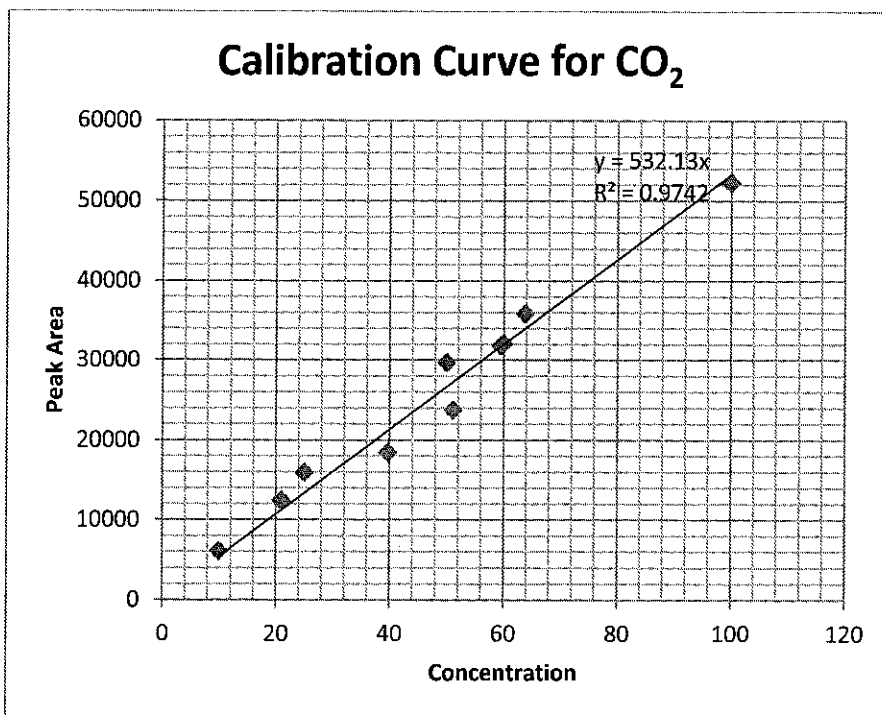


Figure 24: Calibration Curve for Carbon Dioxide

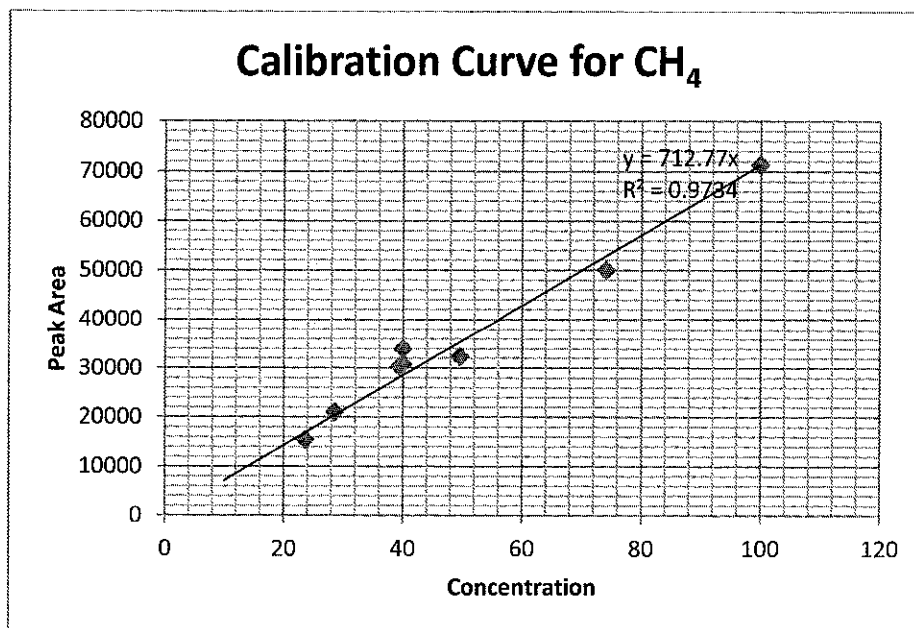


Figure 25: Calibration Curve for Methane



## *Discussion*

The data obtain from the calibration of the gases using the gas chromatograph is important in evaluating and analyzing the unknown outlet sample from the packed bed. As shown from the graph, the retention time for carbon dioxide and methane is different. The retention time for carbon dioxide is around 2.776 minute while the retention time for methane is 2.446 minute. This difference in retention time will allow for qualitative analysis of the unknown sample. The calibration curve obtain from the gas chromatograph however is useful in quantitative analysis of the unknown sample. The external standard is used in the quantitative analysis of the gas using gas chromatograph. The R- squared coefficient obtained from both calibration curve is closer to 1.0, thus the calibration curve is fit to be used for quantitative analysis of the unknown gas mixture sample.

However, care must be taken that the operation and system performance of the GC is stable and consistent. This includes the injection amount, split ratio, oven temperatures, pressures, detector set points, etc. Figure 23 and figure 24 below show the condition of the oven as well as certain parameters that are used for characterization of CO<sub>2</sub> and CH<sub>4</sub>.



Figure 26: The condition set for the gas chromatography

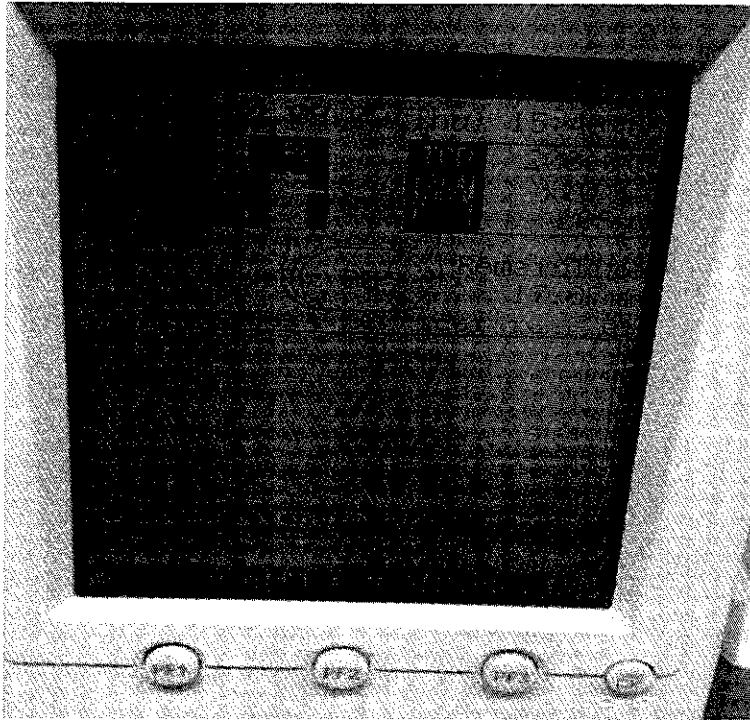


Figure 27: The condition set for the gas chromatography (oven)

**Experiment 2: Obtaining the Void Fraction and Physical Properties of the Bed**

**Void Fraction,  $\epsilon_{bed}$**

Void fraction is the measure of the empty spaces in the material. The void fraction calculated here is the measure of the empty spaces in the packed bed. The void fraction of the bed is calculated using the formula shown below.

$$\text{Void fraction} = \frac{\text{Volume of empty space, } V_e}{\text{Volume with packing, } V_m}$$

The result is presented in the table below:

Table 3: Bed Void Fraction

| Trial                           | 1     | 2     | 3     | 4     | 5     |
|---------------------------------|-------|-------|-------|-------|-------|
| $V_e$ (ml)                      | 1087  | 1080  | 1096  | 1086  | 1088  |
| $V_m$ (ml)                      | 688   | 700   | 682   | 700   | 693.5 |
| Void fraction, $\epsilon_{bed}$ | 0.633 | 0.648 | 0.622 | 0.645 | 0.637 |

Based on the table the average void fraction of the pipe is 0.637.

## Properties of the packed bed

Table 4: Cryogenic Packed Bed Properties

| Packed Bed Properties                 | Data                   |
|---------------------------------------|------------------------|
| Length bed, L                         | 0.46 m                 |
| Diameter bed, D                       | 0.0418 m               |
| Volume of bed, $V_{bed}$              | $0.000645 \text{ m}^3$ |
| Bed void fraction, $\epsilon_g$       | 0.637                  |
| Density of packing material, $\rho_s$ | $2562 \text{ kg/m}^3$  |
| Volume of packing material, $V_s$     | $0.000002 \text{ m}^3$ |
| Diameter of packing material, $d_p$   | 10 mm                  |
| Mass of packing material, $m_p$       | 5.124 g                |

## Discussion

The experiment is repeated several times to obtain the average void fraction of the bed as to get more accurate data. The void bed fraction is obtained to be 0.637. Besides that, data about the properties of the packed bed is also obtained and recorded for future use. The bed void fraction is important in the dynamic packed bed as the empty spaces will be the pathway for the methane gas to flow out of the bed while the  $\text{CO}_2$  is to be deposited on the packing material.

### Experiment 3: Obtaining the Heat Transfer Coefficient of the Bed

The result for experiment 3 is represented in the graph in figure 28 for the study of the heat loss to the surrounding of the system.

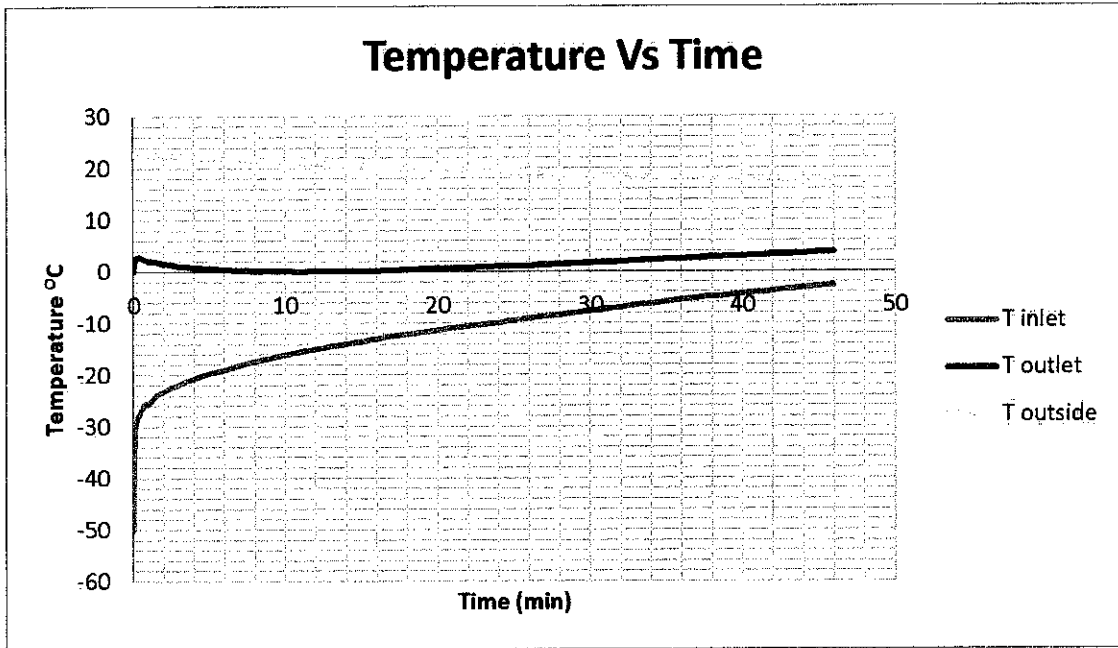


Figure 28: Study of the heat loss to the surrounding of the system.

The graph shows the temperature profile of the bed after the liquid nitrogen supply is stopped. T inlet refers to the temperature probes located closest to the liquid nitrogen supply while the T outlet refers to the temperature probes located further away from the liquid nitrogen supply. T outside refers to the temperature probes located at the outer shell of the 4" pipe which is used as insulation to the cooled packed bed. As we can see from the graph, the temperature of the packed bed dropped rapidly right after the liquid nitrogen supply is stopped. However, the temperature of the packed bed dropped slowly after the rapid drop which is after 10s. This may be due to the system not reaching stability yet. Thus right after 10s, the temperature dropped rapidly. However, we are trying to see the heat loss to the surrounding of the system from this experiment, and we can say that the heat loss is minimal due to the slow dropped in the temperature outside of the 4" pipe. It should be noted that the temperature of the surrounding is 23.5°C and the heat of the outside of the system is 22.8 which is very close to the temperature of the surrounding.

Therefore, the 4" pipe as well as the Hypalon (chlorosulfonated polyethylene (CSPE) synthetic rubber (CSM)) that is used to insulate the pipe is doing a good job in reducing the heat or cold loss to the surrounding. This is due to Hypalon ability to withstand extreme temperature as well as insulating ability.

**Experiment 4: Cryogenic Separation of CO<sub>2</sub>**

The temperature profile obtained from experiment 4 is shown in the graph in figure 29 below:

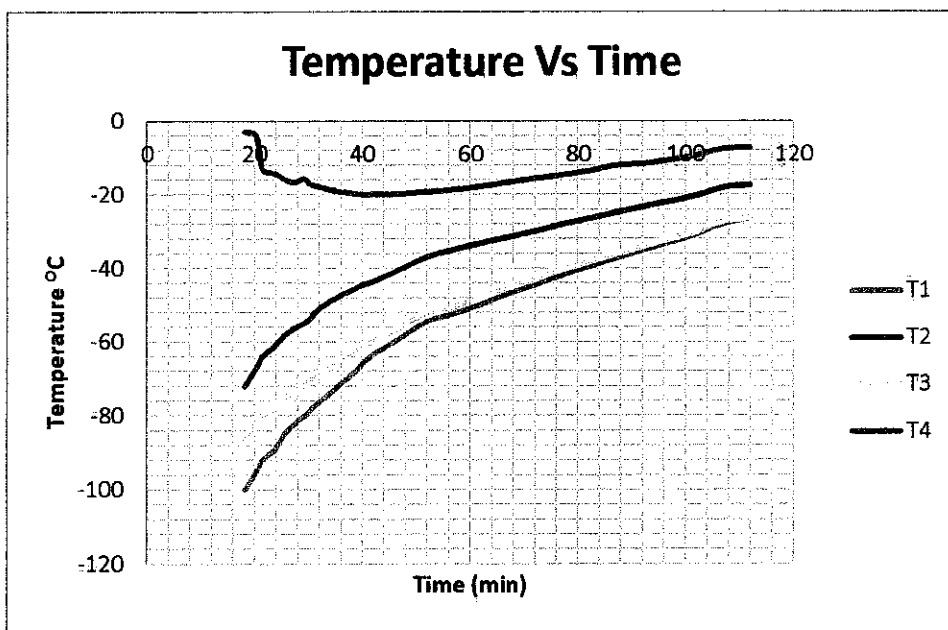


Figure 29: Temperature profile for the CO<sub>2</sub> capture using packed bed.

From the graph, T1 corresponds to the thermometer probes closest to the inlet of liquid nitrogen supply. T2 refers to the thermometer probes located at the end of the packed bed furthest from the liquid nitrogen supply. T3 refers to the thermometer probes located in the middle of the packed bed and T4 refers to thermometer probes located inside the 4" pipe. The location of the probes is shown in the figure 30.

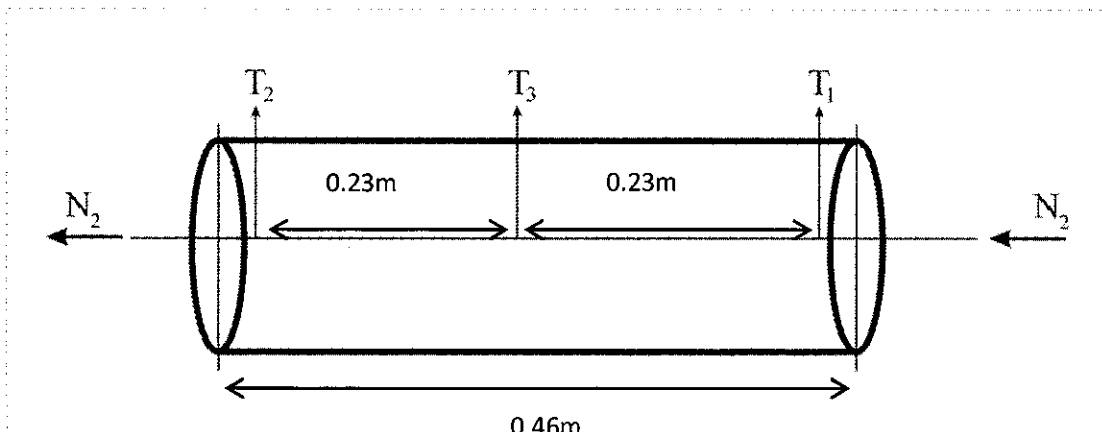


Figure 30: The location of the thermometer probes

The graph shows the slow increase of the temperature of the packed bed after the  $CO_2$  is supplied to the packed bed. This is due to the very low temperature of the bed at the time. However, as the time increases, the temperature of the bed is increasing faster. This is due to the loss of “cold” or the transfer of heat from the higher temperature  $CO_2$  to the very low temperature of the packed bed. However the graph is not able to show the mass deposition of  $CO_2$  in the packed bed as we need to have more temperature probes along the bed to see the better temperature profile.

As mention earlier,  $CO_2$  is supplied at the other end of the packed bed which is closest to  $T_2$ . The  $CO_2$  is supplied in a laminar flow with flow rate  $0.00033 \text{ m}^3/\text{s}$  and  $0.00004 \text{ m}^3/\text{s}$  for case 2.  $CO_2$  is supplied in a laminar flow so as to increase the mass deposition rate of  $CO_2$ . This is because, laminar flow increase the contact of the gas with the packing.

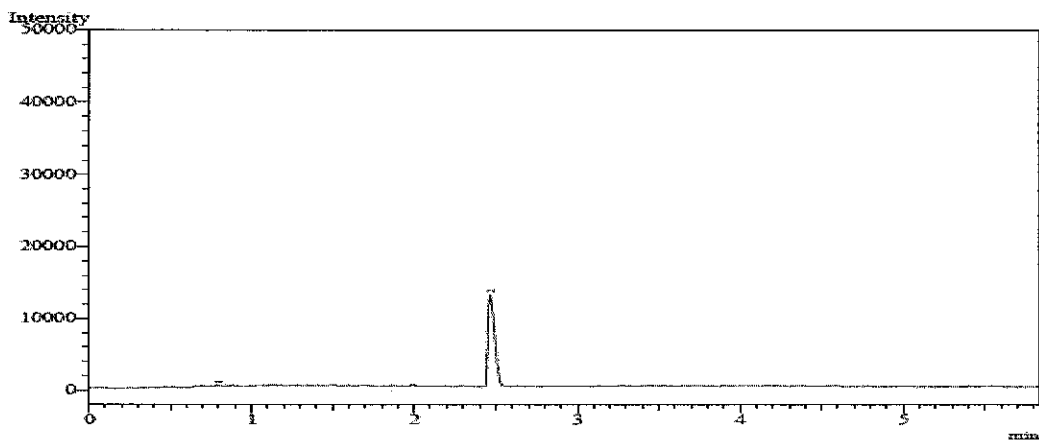
The sample taken from the outlet of the packed bed was analyzed using gas chromatograph. The result is shown in figure 31 for case 1 and 32 for case 2. The sample analysis is provided in the table 5. Figure 31 shows that there are 64.38% of  $CO_2$  that escaped the packed. This means that only 35.62% of  $CO_2$  is captured in the packed bed for case 1. However, for case 2, the result shows that all of the  $CO_2$  is able to be captured by the packed bed. This is due to the slower flow rate of feed during case 2 which gives more time for the  $CO_2$  to contact with the packing material.

Table 5: Result from experiment cryogenic CO<sub>2</sub> capture using packed bed

|        | CO <sub>2</sub> flow rate (m <sup>3</sup> /s) | CO <sub>2</sub> flow rate (L/min) | P (atm) | T1 (°C) | T2 (°C) | T3 (°C) | T4 (°C) | %CO <sub>2</sub> at outlet (%) | Time Sample taken (min) |
|--------|---|-----------------------------------|---------|---------|---------|---------|---------|--------------------------------|-------------------------|
| Case 1 | 0.00033                                       | 20                                | 1       | -90     | -62     | -79     | -16     | 64.38                          | 1                       |
| Case 2 | 0.00004                                       | 2.32                              | 1       | -90     | -55     | -70     | -1.3    | 0                              | 3                       |

CO<sub>2</sub> % at the inlet = 100%

Analysis Date & Time : 14/08/2012 3:51:28 PM Sample Information  
 Sample Name : Unknown 1  
 Sample ID :  
 Data Name : C:\GCsolution\Data\2012\syira\syira\_301.gcd  
 Method Name : C:\GCsolution\Data\2012\syira\new curve 0809.gcm



| Peak# | Ret. Time | Area     | Height   | Conc.   | Units  | Name           |
|-------|-----------|----------|----------|---------|--------|----------------|
| 1     | 1.223     | 1156.27  | 199.15   | 0.0000  |        |                |
| 2     | 2.754     | 34282.84 | 12759.91 | 64.3838 | mole % | Carbon Dioxide |
| Total |           | 35439.11 |          | 64.3838 |        |                |

Figure 31: Gas Chromatography result for case 1.

Analysis Date & Time : 14/08/2012 3:58:15 PM  
 Sample Name : CO2 sample 2  
 Sample ID :  
 Data Name : C:\GCsolution\Data\2012\syira\syira 302.gcd  
 Method Name : C:\GCsolution\Data\2011\vest 01.gcm

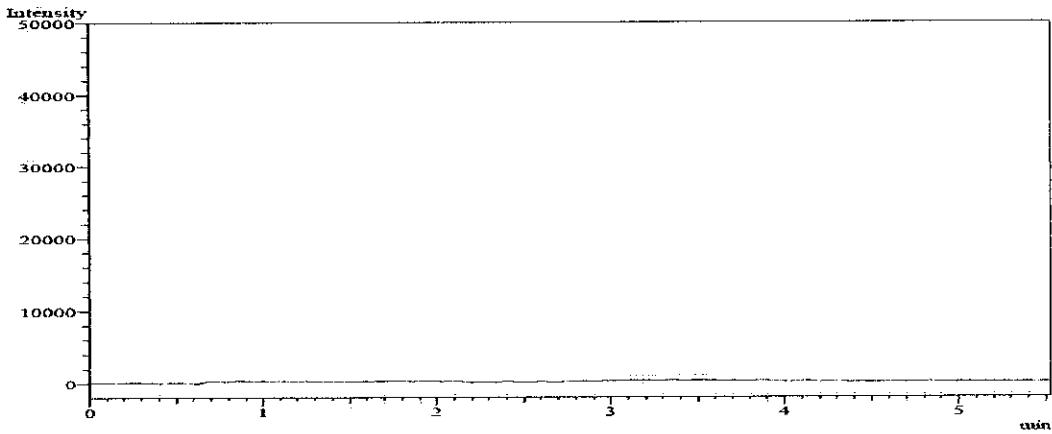


Figure 32: Gas Chromatograph result for case 2

The temperature profile for the experiment cryogenic CO<sub>2</sub> capture using packed bed is shown in figure 33. The figure shows that the temperature of the packed bed is increasing rapidly after feed is introduced into the system compared with the temperature profile of the packed bed heating naturally. This is due to the transfer of heat from the relatively hot feed gas to the cold packing material. Compared with the situation where the packing material is heating up naturally.

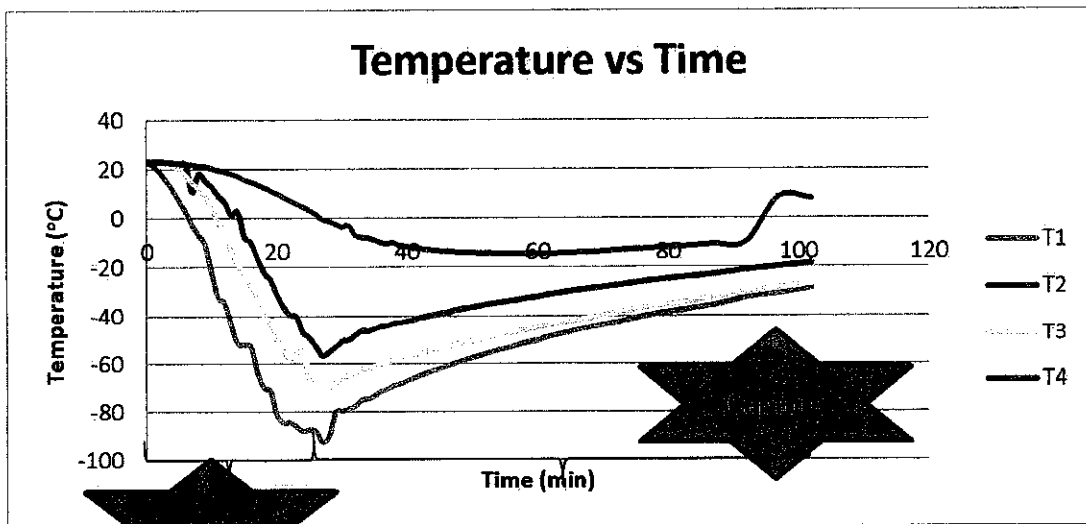


Figure 33: Temperature profile for the CO<sub>2</sub> capture using packed bed with bed composite cooling & capture data.



## **CHAPTER 5**

### **5 CONCLUSION AND RECOMMENDATION**

#### **5.1 RECOMENDATION**

Further optimization and intensification work to enable the use of this technology for offshore application. Besides that, the process is in batch process, therefore, it is best if the process can be converted to the continuous process to ease the application as well as to increase yield and reduce time. Moreover, more experimentation should be done to validate and get a good match with the simulation result. This is because, due to time and equipment constraint, the experiments are not able to be carried out fully which is an issue in the early stages of the project. However, it is recommended to carry out the experimental study using the fabricated experimental apparatus that is used in this project so as to save time.

Moreover, it is recommended to provide a guideline to students on the person in charge to several of equipment and apparatus needed for the laboratory work so that, less time is used to locate the right person and more time is used worthily.

## 5.2 CONCLUSION

The simulation study shows that the  $\text{CO}_2$  is deposited in the bed as the mass fraction of  $\text{CO}_2$  is decreasing with time. Besides that, from the figure 21: mass deposition rate vs temperature, we can see that the higher the concentration of  $\text{CO}_2$ , the higher the mass deposition rate of  $\text{CO}_2$ . This indicates that the potential for the high concentration of  $\text{CO}_2$  to be captured in the packed bed is high for the higher concentration of  $\text{CO}_2$ . Moreover, cryogenic packed bed system used for the experimental study is able to contain the “cold” (extreme low temperature) by minimizing the transfer of heat from the surrounding to the system. Thus, this cryogenic packed bed is suitable to be used for experimental study of cryogenic  $\text{CO}_2$  capture as well as for further experimental study. The calibration curve obtained from the characteristic of  $\text{CO}_2$  is an essential source for the further sample analysis for the experimental study of cryogenic  $\text{CO}_2$  capture which is related to  $\text{CO}_2$  and  $\text{CH}_4$ . Currently it is not possible to simulate the dynamic packed bed experimentally. Thus, the data for the separation of  $\text{CO}_2$  using the dynamic packed bed can be obtained only from the simulation.

As a conclusion, the project to be carried out is a recent technology, more research work need to be done in order to assess the system. Besides that, it is suggested to carry out the experiment for the variation of temperature and pressure to determine the optimum operating condition of the system that is suitable for the  $\text{CO}_2$  – methane system as the current published work is done on the separation of  $\text{CO}_2$  from flue gas.

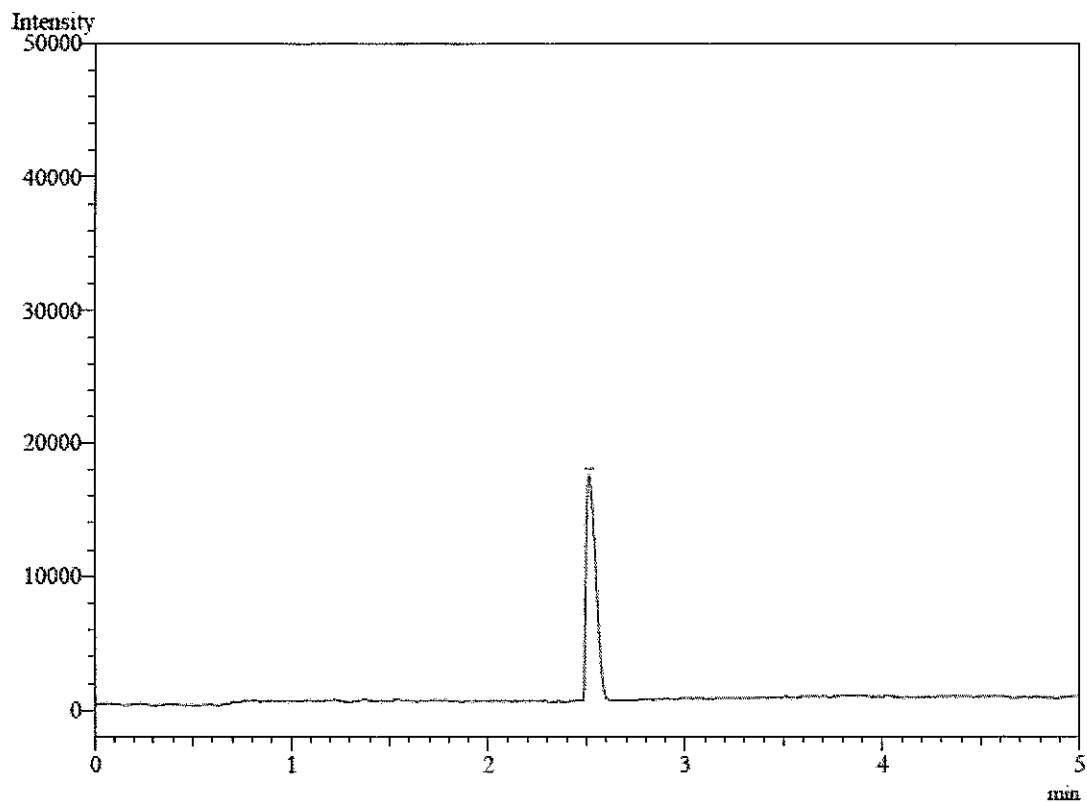
## REFERENCES

- Clodic, D., Younes, M., (2002). A New Method for CO<sub>2</sub> Capture: Frosting CO<sub>2</sub> at Atmospheric Pressure. *Sixth International Conference on Greenhouse Gas Control Technologies, GHGT6*.
- Davidson, J., & Kelly, T. (2004). *Technologies for Capture of Carbon Dioxide*.
- Donnelly, H. G., & Katz, D. L. (1954). Phase Equilibria in the Carbon Dioxide–Methane System. *Industrial & Engineering Chemistry*, 46(3), 511-517.
- Enbenezzer, S. A. (2005). *Removal Of Carbon Dioxide From Natural Gas For Lng Production*. Trondheim: Institute of Petroleum Technology Norwegian University of Science and Technology.
- Fleay, B. J. (2002). *Natural Gas "Magic Pudding" or Depleting Resource*: Water Authority of Western Australia.
- Hart, A., & Gnanendran, N. (2009). *Cryogenic CO<sub>2</sub> capture in natural gas*.
- Keskes, E., Adjiman, C. S., Galindo, A., & Jackson, G. (2006). *A Physical Absorption Process for the Capture of CO<sub>2</sub> from CO<sub>2</sub>-Rich Natural Gas Streams*. London: Chemical Engineering Department, Imperial College London.
- Malaysia, G. (2011). THE FUTURE OF THE GAS INDUSTRY IN MALAYSIA Retrieved 13 March 2012, 2012, from [http://www.gasmalaysia.com/about\\_gas/future\\_gas\\_industry.htm](http://www.gasmalaysia.com/about_gas/future_gas_industry.htm)
- Song, C.-F., Kitamura, Y., Li, S.-H., & Ogasawara, K. (2012a). Design of a cryogenic CO<sub>2</sub> capture system based on Stirling coolers. *International Journal of Greenhouse Gas Control*, 7(0), 107-114.
- Tuinier, M. J., van Sint Annaland, M., Kramer, G. J., & Kuipers, J. A. M. (2010). Cryogenic capture using dynamically operated packed beds. *Chemical Engineering Science*, 65(1), 114-119.
- Tuinier, M. J., van Sint Annaland, M., Kramer, G. J., & Kuipers, J. A. M. (2010). Cryogenic CO<sub>2</sub> Capture Using Dynamically Operated Packed Beds. *Chemical Engineering Science*.
- Fonseca, D. A. (2012). Perkin Elmer Autosystem Gas Chromatograph. from <http://www2011.energy.psu.edu/sp/facilities/tcdDetection.html>
- ExxonMobil. (2010). Controlled Freeze Zone™ increasing the supply of clean burning natural gas. Irving, Texas: ExxonMobil.
- Panahi, M. (2011). Cryogenic CO<sub>2</sub>/H<sub>2</sub>S capture technologies for remote natural gas processing. In N. U. o. S. a. Technology (Ed.). Trondheim.
- Stepan, D. J. (2009). *Mitigation of Hydrogen Sulfide with Concomitant Enhancement of Microbial Methane Production in Biomass Digesters*. North Dakota: University of North Dakota.

## APPENDIX

### Result for Experiment 3: Obtaining the Calibration Curve for the CO<sub>2</sub> and CH<sub>4</sub> Mixture Using Gas Chromatograph

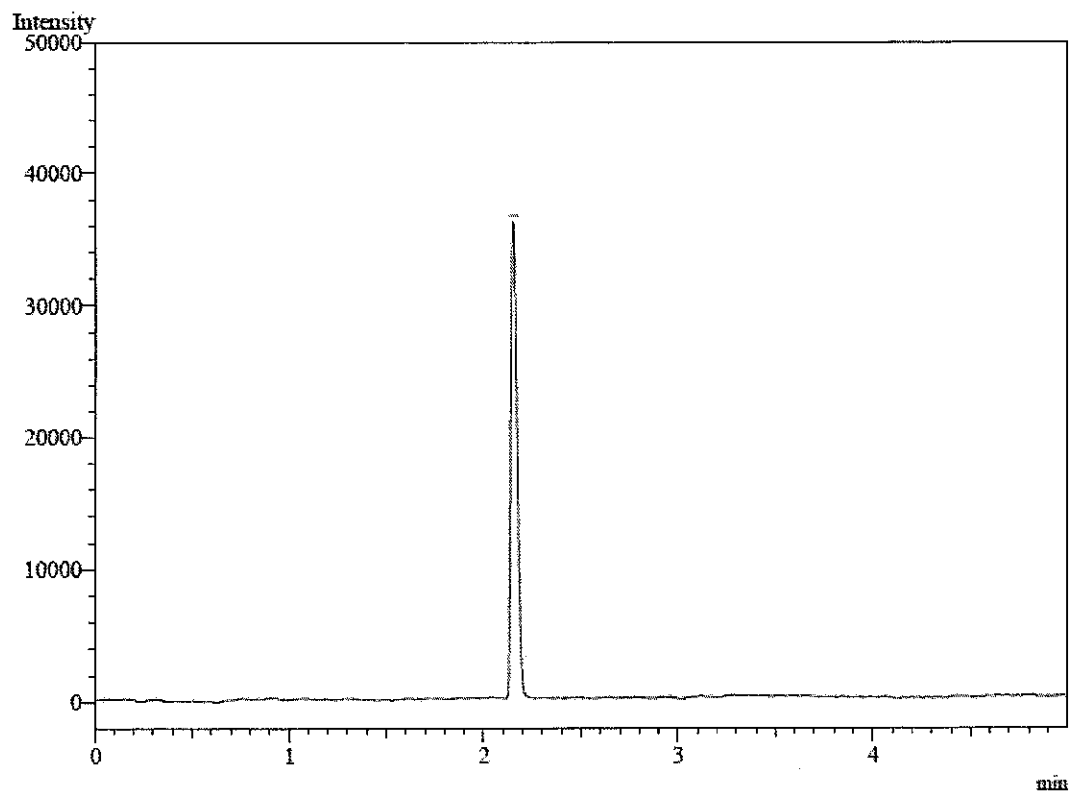
Sample Name : Carbon dioxide  
Sample ID :  
Data Name : C:\GCsolution\Data\2012\syira\syira 01.gcd  
Method Name : C:\GCsolution\Data\2012\syira\calibration.gcm



| Peak#        | Ret. Time | Area     | Height   | Conc.    | Units | Name           |
|--------------|-----------|----------|----------|----------|-------|----------------|
| 1            | 2.761     | 52192.07 | 16882.16 | 100.0000 | %     | Carbon Dioxide |
| <b>Total</b> |           | 52192.07 |          | 100.0000 |       |                |

Figure 1: Calibration Curve for pure Carbon Dioxide

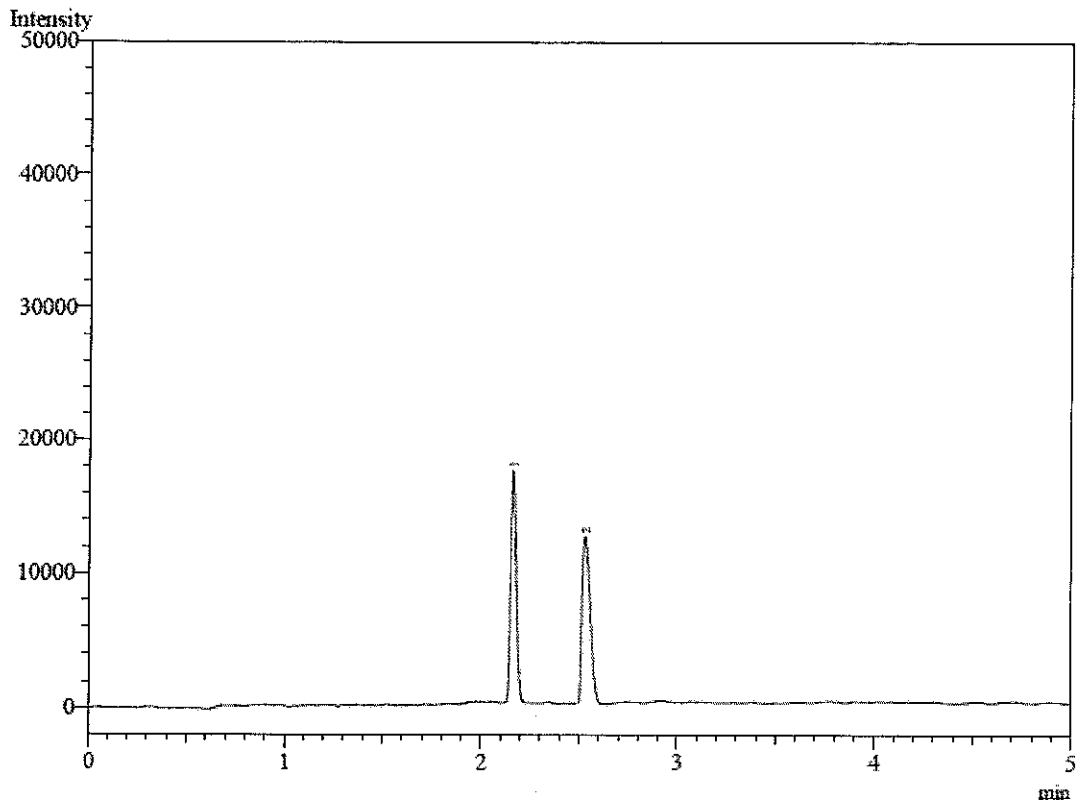
Sample Name : Methane  
 Sample ID :  
 Data Name : C:\GCsolution\Data\2012\syira\syira 02.gcd  
 Method Name : C:\GCsolution\Data\2012\syira\calibration.gcm



| Peak#        | Ret. Time | Area     | Height   | Conc.    | Units | Name    |
|--------------|-----------|----------|----------|----------|-------|---------|
| 1            | 2.437     | 71275.98 | 35852.40 | 100.0000 | %     | Methane |
| <b>Total</b> |           | 71275.98 |          | 100.0000 |       |         |

Figure 2: Calibration Curve for pure Methane

Sample Name : 60% CO2 + 40% CH4  
 Sample ID :  
 Data Name : C:\GCsolution\Data\2012\syira\syira 03.gcd  
 Method Name : C:\GCsolution\Data\2012\syira\calibration.gcm



| Peak#        | Ret.Time | Area            | Height   | Conc.           | Units | Name           |
|--------------|----------|-----------------|----------|-----------------|-------|----------------|
| 1            | 2.446    | 30663.30        | 17242.20 | 40.0000         | %     | Methane        |
| 2            | 2.776    | 32048.88        | 12450.84 | 60.0000         | %     | Carbon Dioxide |
| <b>Total</b> |          | <b>62712.18</b> |          | <b>100.0000</b> |       |                |

Figure 3: Calibration Curve for 40% Methane and 60% Carbon Dioxide